Published in final edited form as:

ACS Biomater Sci Eng. 2023 December 11; 9(12): 6586–6609. doi:10.1021/acsbiomaterials.3c01171.

3D Printing Applications for Craniomaxillofacial Reconstruction: A Sweeping Review

Blaire V. Slavin,
University of Miami Miller School of Medicine, Miami, Florida 33136, United States

Quinn T. Ehlen,
University of Miami Miller School of Medicine, Miami, Florida 33136, United States

Joseph P. Costello II,
University of Miami Miller School of Medicine, Miami, Florida 33136, United States

Vasudev Vivekanand Nayak,
Department of Biochemistry and Molecular Biology, University of Miami Miller School of Medicine, Miami, Florida 33136, United States;

Estavam A. Bonfante,
Department of Prosthodontics and Periodontology, University of Sao Paulo, Bauru School of Dentistry, Bauru, São Paulo 17012-901, Brazil

Ernesto B. Benalcázar Jalkh,
Department of Prosthodontics and Periodontology, University of Sao Paulo, Bauru School of Dentistry, Bauru, São Paulo 17012-901, Brazil

Christopher M. Runyan,
Department of Plastic and Reconstructive Surgery, Wake Forest School of Medicine, Winston-Salem, North Carolina 27101, United States

Lukasz Witek,
Biomaterials Division, NYU Dentistry, New York, New York 10010, United States; Hansjörg Wyss Department of Plastic Surgery, NYU Grossman School of Medicine, New York University, New York, New York 10017, United States; Department of Biomedical Engineering, NYU Tandon School of Engineering, Brooklyn, New York 11201, United States;

Paulo G. Coelho
Department of Biochemistry and Molecular Biology, University of Miami Miller School of Medicine, Miami, Florida 33136, United States; DeWitt Daughtry Family Department of Surgery, Division of Plastic Surgery, University of Miami Miller School of Medicine, Miami, Florida 33136, United States

Corresponding Author: Vasudev Vivekanand Nayak – Department of Biochemistry and Molecular Biology, University of Miami Miller School of Medicine, Miami, Florida 33136, United States; vxn188@miami.edu.

Author Contributions

B.V.S.: Investigation, Writing–original draft, Visualization. Q.T.E.: Investigation, Writing - original draft, Visualization. J.P.C.: Visualization. V.V.N.: Writing–review and editing. E.A.B.: Writing–review and editing. E.B.B.J.: Writing–review and editing. L.W.: Conceptualization, Writing–review and editing. P.G.C.: Conceptualization, Writing–review and editing.

The authors declare no competing financial interest.

Complete contact information is available at: https://pubs.acs.org/10.1021/acsbiomaterials.3c01171

Abstract

The field of craniomaxillofacial (CMF) surgery is rich in pathological diversity and broad in the ages that it treats. Moreover, the CMF skeleton is a complex confluence of sensory organs and hard and soft tissue with load-bearing demands that can change within millimeters. Computer-aided design (CAD) and additive manufacturing (AM) create extraordinary opportunities to repair the infinite array of craniomaxillofacial defects that exist because of the aforementioned circumstances. 3D printed scaffolds have the potential to serve as a comparable if not superior alternative to the "*gold standard*" autologous graft. *In vitro* and *in vivo* studies continue to investigate the optimal 3D printed scaffold design and composition to foster bone regeneration that is suited to the unique biological and mechanical environment of each CMF defect. Furthermore, 3D printed fixation devices serve as a patient-specific alternative to those that are available off-the-shelf with an opportunity to reduce operative time and optimize fit. Similar benefits have been found to apply to 3D printed anatomical models and surgical guides for preoperative or intraoperative use. Creation and implementation of these devices requires extensive preclinical and clinical research, novel manufacturing capabilities, and strict regulatory oversight. Researchers, manufacturers, CMF surgeons, and the United States Food and Drug Administration (FDA) are working in tandem to further the development of such technology within their respective domains, all with a mutual goal to deliver safe, effective, cost-efficient, and patient-specific CMF care. This manuscript reviews FDA regulatory status, 3D printing techniques, biomaterials, and sterilization procedures suitable for 3D printed devices of the craniomaxillofacial skeleton. It also seeks to discuss recent clinical applications, economic feasibility, and future directions of this novel technology. By reviewing the current state of 3D printing in CMF surgery, we hope to gain a better understanding of its impact and in turn identify opportunities to further the development of patient-specific surgical care.

Graphical Abstract

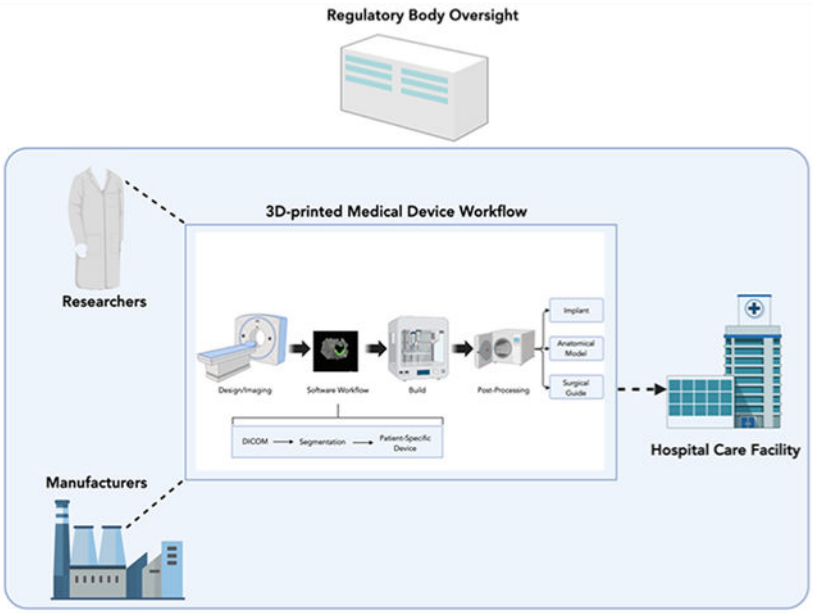

Keywords

3D printed medical devices; additive manufacturing; craniomaxillofacial surgery; biomaterials; bone regeneration; FDA regulation

1. INTRODUCTION

A large portion of our self-identity is housed within facial features. Patients with facial differences as a result of craniomaxillofacial (CMF) trauma, such as sports injuries and road accidents, congenital anomalies, infectious disease, tumor resection, or edentulism have reported associated stressors of self-acceptance, negative responses of others, and difficulty coping with associated impairments.[1–4] These associated impairments can include compromised sensory organ function, speech, and mastication.[5] The field of CMF surgery treats a diverse range of ages and pathologies, both of which must be considered when CMF surgeons form and execute their surgical plan. Moreover, the CMF surgeon is challenged by varying load-bearing demands, proximity of sensory organs, as well as the microbiota of the oronasal cavity, all of which may complicate bone healing.[6] A multitude of strategies to fit and fill these defects have been deployed and continue to evolve in the hope of restoring the form and function of any given defect site. The combined effort of computer-aided design/computer-aided manufacturing (CAD/CAM) and 3D printing (3DP) to create patient-specific devices based on individual computed tomography (CT) or magnetic resonance imaging (MRI) data is one such strategy that has drastically changed the approach to CMF defect repair.

Traditionally, CMF reconstruction relies upon harvesting bone from a healthy donor site such as the fibula. While autografting remains the gold standard today, it is limited by donor site morbidity, finite stock, risk of resorption, prolonged operative time and hospital stay, as well as patient-reported increases in postoperative pain.[7–9] Allografts and xenografts solve many of the autograft's shortcomings, yet they are still associated with risk of disease transmission and antigenic reactions.[7,10] For these reasons, synthetic alloplasts, including metals, polymers, and ceramics, have been popularized within the field of CMF. The characteristics of any implantable material, resorbable or nonresorbable, should meet the needs of the biological environment it is placed within. For non-resorbable materials traditionally used for rigid fixation (e.g., titanium alloys), these needs include biocompatibility, mechanical strength, and osteogenic properties that facilitate bone healing, at a minimum. While this is equally as important for resorbable materials used in other forms of bone defect repair (e.g., ceramics and many synthetic polymers), they are also expected to degrade in a predictable and timely manner such that the defect site is mechanically supported as the material gradually becomes replaced with regenerated bone that is similar in quality to native bone.[11,12,10] This is achievable only if the material is pro-osteogenic, pro-angiogenic, and inflammation from its degradation is kept to a minimum so as to not interfere with any of these processes. A material that meets these requirements does not currently exist without the combined effort of bone tissue engineering strategies and three-dimensional (3D) printing.

With respect to conventionally used fixation devices, commercially available plates are produced in generalizable configurations, requiring the surgeon to manually bend them to a contour specific to the patient's anatomy. They typically need to be adjusted again intraoperatively as changes to surgical margins may occur between the preoperative and intraoperative period.[13] This can be physically challenging and time-consuming to the point that it significantly extends operative time, particularly for surgeons early on in their training.[13–15] Even still, complete bone-plate congruence without visible gaps is rarely achieved.[13,16] For more complicated cases, a plate may need to be bent repeatedly, resulting in residual stresses that can compromise its performance *in vivo*.[13,14,17–19] Residual stresses generated from titanium plate contouring have been theorized to initiate crack formation that then grow larger under the loading stresses associated with mastication, leading to plate fracture and screw loosening.[13,17,19] Previous literature has found that in comparison to commercial plates made of the same material, 3D printed plates have superior mechanical properties.[14] Furthermore, the need to bend 3D printed plates preoperatively may be minimized or eliminated, as they are printed to fit the exact shape of patient anatomy. This shortens operative time and reduces any unnecessary wear that may compromise performance.[14,20]

In addition to fixation devices, 3D printing can be utilized to create other implantable and nonimplantable devices to improve CMF surgical care. Implantable scaffolds for bone defect repair are customizable to the nanoscale allowing them, unlike autografts, to precisely fit geometrically complex defects.[16,21–23] Alterations to scaffold architecture, including porosity and surface topography, lends to both augmented osteoconductivity and vascularization within defects.[10,24] Moreover, scaffolds may be further seeded and/or coated with mesenchymal stem cells, exogenous growth factors, antimicrobials, and regenerative pharmaceuticals to minimize risk of failure and further accelerate bone growth and neoangiogenesis.[10,25–27] Other uses for 3D printing within craniofacial surgery are patient-specific anatomic models or surgical guides for preoperative and intraoperative use. Clinical studies have found overwhelming evidence of improved surgical accuracy and aesthetic outcomes.[28–31]

However, patient-specific 3D printed medical devices (3DMD) are still in their nascency, with many barriers to overcome before they become commonplace in the operating room. The aim of our review is to comprehensively assess the role of 3D printing in craniomaxillofacial reconstruction. The FDA regulatory status of 3DMD, as well as 3D printing techniques, biomaterials, and sterilization procedures suitable for 3DMD of the CMF skeleton are discussed. Finally, recent clinical applications, economic feasibility, and future directions of this novel technology are examined.

2. FDA REGULATORY OVERSIGHT

Attaining FDA approval of patient-specific 3D printed medical devices, whether for anatomical model, surgical guide, or implantable scaffold, is a complex feat. 3DMD devices are regulated by the FDA's Center for Medical Devices and Radiological Health (CDRH). 3DMD with biologic components (i.e., stem cells and exogenous growth factors) are termed "combination products" and require the additional involvement of the Center

for Biologics Evaluation and Research (CBER), adding further scrutiny/complexity to the approval process. This has led to the creation of the Breakthrough Device Program which aims to expedite the development, assessment, and review of combination products if they meet certain criteria.[32] It is paramount that researchers determine what regulatory agency their device falls under, as this will dictate which regulations they must follow. Researchers should also anticipate any resistance that they may meet regarding their development process in the early stages of experimentation to accelerate future clinical applicability.[33] Furthermore, gaining a deeper understanding of this rigorous process will allow craniomaxillofacial surgeons to effectively deliver safe, innovative, and informed care to their patients.

The U.S. FDA seeks to align its quality system (QS) requirements for medical devices with those of the International Organization for Standardization (ISO). The ISO is a nongovernmental global network of national standards bodies; of which, the American National Standards Institute (ANSI) serves as the U.S. member body to the ISO. QS requirements for FDA-regulated medical devices are called current good manufacturing practices (CGMP) and can be found in part 820 under section 520(f) of the Federal Food, Drug and Cosmetic Act.[34] They are intended to provide a framework of basic requirements that manufacturers must abide by in their production process of medical devices for human use.[34] Manufacturers only need to follow those that are applicable to their specific device.[34] For QS regulation of a device constructed with additive manufacturing, QS requirements must be enforced at each phase of development. The set of ISO standards that are related to medical device biocompatibility is ISO 10993. Standards that fall within the scope of ISO 10993 are often referenced in FDA guidance documents for medical device manufacturers. Furthermore, the ISO technical committee (TC) responsible for publishing standards related specifically to additive manufacturing is called ISO/TC 261.

As characterized by the FDA, the additive manufacturing process of a medical device can be divided into five phases: design, software workflow, build, postprocessing, and final testing considerations (Figure 1A).[33] In the design phase, patient CT or MRI data are converted to a compatible format (e.g., DICOM file).[35] During the software workflow phase, the scan is segmented by an image segmentation system, such that the anatomical region of interest is isolated from the remainder of the scan. It can then be further optimized prior to conversion to a 3D printer compatible file (e.g., standard triangulation language (STL) file). Many patient-specific implants for cranial defects are designed using the mirror image reconstruction technique, where the healthy side contralateral to the defect is mirrored along the midsagittal plane.[15] This technique becomes problematic if the defect crosses the midsagittal line. An alternate technique, called the baffle planner technique, does not require an intact contralateral side to model the implant.[15] As a part of the build phase, selected materials are used to fabricate the device. Postprocessing may consist of, but is not limited to, cleaning unsintered raw materials, sterilization, packing, and labeling. The device can only then be tested and characterized (e.g., geometry, dimensions, mechanical properties) in its final form, after postprocessing, in what is known as the final testing considerations phase. Ultimately, any 3DMD device to be sold and marketed should be prepared using FDA-cleared segmentation software, printer, materials, and postprocesses.[35] An overview of

considerations to address within each part of the 3DMD workflow is illustrated in Figure 1B.

The FDA classifies medical devices into the following regulatory classes, Class I, II, and III. Assigned rank of a device is determined by degree of risk posed to the patient and intended use and specialized indications for use. Consequently, class rank determines the type of premarket submission required for FDA clearance to market.[37] Class I and II devices, unless exempt, will require the submission of a premarket notification, also known as a 510(k). A class I or II device cannot be marketed until the FDA issues a 510(k) clearance stating that the device is substantially equivalent (SE) to an existent, FDA-approved predicate device.[38] A study published in 2018 performed a search of the FDA medical device database that determined 7% of 3DMD cleared through the 510(k) pathway thus far were for craniofacial application.[39] And as of 2023, only five 3DP software platforms (class II devices) currently on the market have been FDA-cleared to create anatomical models specifically for craniomaxillofacial reconstruction.[35] The companies that produce the 510(k)-cleared software include Materialise, 3D systems, Ricoh, Axial 3D, and Medviso.[35] For class III devices, a premarket approval application (PMA) is necessary. This is typically required if the device is new or if a device submitted through a 510(k) is deemed not substantially equivalent (NSE) to a predicate.[40] A PMA for a class III device necessitates submission of scientific evidence in support of clinically significant results with benefits that outweigh any associated risks of its use.[40] Moreover, whether the 3DMD is implantable, load-bearing, or patient-specific will also impact the type of information that should be included to establish device safety and efficacy in any given premarket submission. The CDRH and CBER can be contacted during the presubmission process for feedback regarding any component of the development process.[33]

To better understand this complex topic, we present the following real-world example. In 2015, BioArchitects submitted a 510(k) premarket notification to the CDRH for FDA approval of a class II, 3DMD device.[41] Their 3D printed titanium cranioplasty plate was deemed substantially equivalent to an existing, legally marketed predicate device used for the same purposes.[42] Thus, the FDA granted them permission to market their device as seen on their Web site,[43] eliminating the need to complete a PMA. It is important to note that data pertaining to any FDA-cleared medical device are accessible in the FDA's online "medical device databases" and can be searched by application route (e.g., 510(k), PMA) or device name.[44]

A massive barrier to 3DMD currently is transporting them safely and in timely to the hospital care facility (HCF). The FDA has begun discussions with stakeholders to determine a regulatory approach that will allow these 3DMD to be manufactured closer to their end-user, the patient, at the point-of-care (POC). Three different POC scenarios have been proposed including (1) HCF use of a 3D printing medical device production system (MDPS), (2) traditional manufacturer on or near the HCF, and (3) 3D printing facility is created and run by the HCF.[45] In scenario 1, an FDA-cleared MDPS, which is a legally marketed bundle of materials, software, printer, and postprocessing equipment intended to create a 3DMD for an intended use (e.g., polymer-based cranioplasty plate), would be located in the HCF. QS regulatory compliance would ultimately fall on the manufacturer

of the MDPS as long as the HCF uses the MDPS in accordance with its labeled use. In scenario 2, the HCF leases space to a traditional manufacturer of a finished device, who would be responsible for regulatory compliance of a given FDA-cleared 3DMD intended for a specific use. Scenario 3 would transfer the responsibilities of QS regulatory compliance entirely to the hands of the HCF. In this case, clinical and engineering training programs for 3DMD development may become a part of certification and licensing programs for surgeons that will frequently use this technology in their practice. Ultimately, the FDA will modify existent and/or formulate new regulations as the technology evolves and regulatory compliance is passed from traditional manufactures to the HCF. For this reason, it is of utmost importance that CMF surgeons become familiar with this process as point-of-care 3D printing facilities trend toward finding a commonplace within hospital systems.

3. BIOMATERIALS FOR 3D PRINTED BONY DEFECT REPAIR OF THE CMF SKELETON

3.1. Titanium and Titanium Alloys.

Titanium is the leading 3D printed biomaterial for craniomaxillofacial repair.[46] More specifically, it is the gold standard for rigid fixation of craniofacial fractures.[46] Direct Metal Laser Sintering (DMLS) or Electron Beam Melting (EBM) are utilized to generate customizable implants for orbital, mandibular, and cranial reconstruction.[47] Titanium and its alloys, classified as a-, (a + b)-, and b-type, are known to exhibit excellent tensile strength while remaining lightweight.[21,29] They are inherently osteointe-grative, facilitating bone growth into the implant; this is theorized to due to an early transition from proinflammatory (M1-phenotype) to reparative/anti-inflammatory (M2-phenotype) macrophage predominance shortly after placement.[29,48–50]

Additionally, the surface layer of titanium-based implants forms an oxide film that is resistant to corrosion.[21] A drawback of this biomaterial is the discrepancy in Young's moduli (i.e., elastic modulus) between titanium alloys and cortical bone, leading to a phenomenon known as stress shielding.[51] Stress shielding, due to differences in moduli between bone and titanium, is a cause of progressive implant loosening, often necessitating reoperation. Interestingly as a class, b-type titanium alloys exhibit the lowest elastic moduli, yet a- and (a + b)-type alloys are more widely used in practice.[51,52] In addition, micro- or nanoscale wear particles from titanium implants have been shown to dampen osteoblastic activity and augment osteoclast recruitment, further perpetuating the issue.[53,54] Investigations continue to (a) engineer b-type titanium alloys with both maximized dynamic strength and a Young's modulus similar to native bone and (b) determine a surface treatment (e.g., abrasive smoothening and polishing, gritting, cold treatment, or passivation and anodization) that would generate a 3D printed surface topography to counteract potential loosening or migration.[24,47,51] There is also risk of susceptibility artifact with various imaging modalities when considering titanium implant placement.[55,56] When imaged with CT or CBCT, metal implants often result in beam hardening, streak artifact, and photon starvation, all of which obscure surrounding structures.[57,58] Furthermore, signal loss, geometric distortion and "pile-up" artifacts often impede MRI imaging if metal implants are present.[59] For these reasons, metal-free implants may be preferable in patients undergoing

oncologic reconstruction, in which complete and accurate visualization of bone and soft tissue structures in the postoperative period is critical.[55] Shared complications of titanium-based implants in all CMF patients (i.e., adult and pediatric) that increase the risk of reoperation include postoperative pain, palpability, infection, and exposure. In this context, 3D printed synthetic polymers have become increasingly popularized as they provide self-limited rigid fixation with a lesser chance of requiring a second procedure.[60,61]

3.2. Synthetic Polymers.

Biocompatible synthetic polymers that are under investigation or currently in use for craniofacial reconstruction include polycaprolactone (PCL), polylactic acid (PLA), polyglycolic acid (PGA), polylactide-*co*-glycolide (PLGA), poly(methyl methacrylate) (PMMA), polyethylene (PE), and polyetheretherketone (PEEK). Synthetic polymers are easily manufactured and cost-effective.[62] Among them, PMMA, PE, and PEEK are nondegradable polymers.[63] Unlike titanium alloys, the appeal of the remaining degradable polymers is that they will not restrict growth in developing pediatric skeletal defects.[60,61,64] Moreover, synthetic polymers do not interfere with radiographic, CT, or MRI studies.[65] They are also lighter than titanium alloys, with fewer reports of pain and palpability.[66] However, synthetic polymers do not possess osteointegrative properties due to their biological inertness.[67] Additionally, elastic moduli of synthetic polymers are generally lower than those of native bone. While this eliminates the concern for stress shielding, it also implies a lessened load-bearing capacity.[5,65] Figure 2A–C represent the Von Mises stress distribution during mastication at single bite points (canine, first molar, second/3rd molar), as determined by finite element models of the human cranium performed by Prado et al.[68] Areas under high stress, as depicted in red, would require materials with high mechanical performance.[68] Scaffolds composed entirely of a synthetic polymer may inadequately support a bony defect at these points while bone regeneration transpires. For these reasons, they are often combined with other biomaterials or bioactive molecules to improve their mechanical strength and bone regenerative capacity, respectively. Some of which have been previously studied include bone-derived mesenchymal stem cells, adipose-derived mesenchymal stem cells (ASCs), stromal vascular fraction (SVF), decellularized cortical bone (DCB), polydopamine, tricalcium phosphate (TCP), hydroxyapatite (HA), gelatin, and collagen.[69–76] A higher rate of infection is also a frequently reported concern of synthetic polymer-based implants.[77] To minimize infection, bactericidal-coated scaffolds continue to be investigated and optimized (e.g., silver nanoparticle impregnation, zinc chelation, ε-Polylysine coating).[78–81] Despite many commonalities among synthetic polymers, each differs in its hydrophilicity, degradation rate, and biocompatibility, impacting their individual potential for clinical application.

3.2.1. Polycaprolactone.—Polycaprolactone, an FDA-ap-proved thermoplastic polyester, is the second most studied and used 3D printed material for craniofacial application.[12,75,76,82–87] PCL is known to be biodegradable and highly biocompatible.[21] PCL is commonly 3D printed using Fused Deposition Modeling (FDM), rendering it very cost-effective.[21] Due to its hydrophobicity, the degradation rate *in vivo* is estimated to occur between 1 and 2 years.[88] This prolonged resorption time may interfere with proper bone regeneration within the defect site if a shorter healing period is expected. For this reason,

PCL has been successfully copolymerized with hydrogels, like collagen, to augment its resorption kinetics while still providing the scaffold great mechanical strength.[89,90] The addition of collagen also improves the scaffold's osteoconductive properties, which are lessened if PCL is used alone. Furthermore, several composite PCL-mineral scaffolds have been compared to evaluate potential osteointegrative enhancement. Mineral sources included HA, TCP, DCB, and Bio-Oss (BO) which is an inorganic bovine trabecular bone. Among all treatment groups, PCL-DCB and PCL-BO demonstrated the greatest osteoinductivity after 3 weeks *in vitro* which was theorized to be due to the presence of a collagen phase.[75]

PCL has also been evaluated as a candidate for craniofacial defect repair in several *in vivo* studies.[86,91] Recently, the effect of oxygen loading on vascularization and bone regeneration was evaluated in critical-sized calvarial defects of a murine model.[86] Biodegradable synthetic microtanks housed within a porous ASC-seeded PCL-scaffold were hyperbarically loaded with pure oxygen. The microtanks were designed to release oxygen over hours after placement *in vivo*. Compared to non-O_2-loaded scaffolds, O_2-loaded scaffolds exhibited enhanced bone regeneration after 8 weeks.[86] O_2-loading may serve as a viable strategy in improving the hypoxic microenvironment known to exist within large nonvascularized scaffolds (>1 mm).[86] Additionally, a study performed by Singh et al. in a skeletally mature minipig model examined the bone regenerative capacity of PCL-DCB scaffolds that were intraoperatively infused with the autologous stromal vascular fraction (SVF) in critical-sized zygomatic arch defects. SVF is an easily accessible and readily available source of mesenchymal stem cells that can be extracted from autologous lipoaspirate tissue. Compared to acellular PCL-DCB scaffolds, the SVF group demonstrated superior osteointegration after 1-year *in vivo*, as deduced by requiring a significantly higher torque to fracture the bone-scaffold interface.[91] This approach to bone regeneration is particularly appealing because, if clinically translated, the SVF could be harvested and extracted intraoperatively from patient's adipose tissue. Moreover, as an autologous cell source with osteogenic potential, SVF-infused scaffolds may supply the benefits associated with an autograft without the comorbidities.

3.2.2. Polylactic Acid, Polyglycolic Acid, Polylactide-co-glycolide.—Polylactic acid, polyglycolic acid, and polylactide-*co*-glycolide are FDA-approved, biodegradable thermoplastic polyesters. PLA and PGA are both hydrolyzed to nontoxic, although acidic products. Local inflammatory responses (LIR) because of their metabolization have been previously reported.[11,92,93] This is of particular importance because inflammation often potentiates fibrosis which may compromise regenerated tissue function or even result in scaffold rejection.[23] Of note, implants placed in anatomical areas with little vascularization are at higher risk of LIR.[94] PLA is a stiff, hydrophobic polymer with an estimated degradation time of 6–24 months.[95,96] By contrast, PGA is more hydrophilic in nature and thus degrades rather rapidly within 1.5–3 months.[95,96] For this reason, PGA-fabricated scaffolds may not adequately provide mechanical support to a defect site while tissue regeneration occurs.[97] However, due to a similar elastic modulus to cortical bone, PGA remains an excellent candidate for bone regeneration if copolymerized with other biomaterials. PLA and PGA can be copolymerized, forming PLGA, to better suit the biological environment. The degradation rate of a PLGA-scaffold can be customized with

molecular weight and PLA:PGA ratio adjustments.[92,96] For example, PLGA (LA/GA = 50/50) will degrade over 1 month, as opposed to PLGA (LA/GA = 85/15) which resorbs completely after 5–6 months due to a higher composition of hydrophobic PLA.[96] Thus far, preclinical studies utilizing 3D printed scaffolds fabricated with PLA, PGA, or PLGA have demonstrated promising results for CMF defect repair.[98–100]

3.2.3. Poly(methyl methacrylate).—Poly(methyl methacrylate) is a nondegradable thermoplastic polyester. PMMA is hydrophobic with mechanical and elastic strength comparable to bone.[101] PMMA commonly serves as an alternative to autografting for cranioplasty. Historically, liquid PMMA was poured directly into a defect to fit and fill it intraoperatively. Consequently, an exothermic hardening process occurred with an associated risk of local tissue necrosis.[102–104] Risk of burn injury is circumvented when PMMA is poured into a 3D printed mold of the defect intraoperatively or 3D printed as a porous PMMA-scaffold preoperatively. While autografting remains the gold standard in cranioplasty today, there is a wealth of evidence that autografts carry greater risk of resorption and failure.[102,105] In this context, alloplastics, such as titanium and PMMA, have been looked at more favorably. That being said, PMMA-fabricated scaffolds have yet to be FDA-cleared for use in cranioplasty due to very low quality of evidence about risk of infection.[101,106] More recently, 3D printed PMMA scaffolds have been successfully applied to midface and mandibular osseous defect repair with low infection rates.[107]

3.2.4. Polyethylene.—Polyethylene is a nondegradable, inexpensive thermoplastic polymer that is often printed with Fused Deposition Modeling (FDM). In comparison to pure PE, high-density polyethylene (HDPE) is more frequently seen in clinical practice due to its superior durability and higher melting point (131 °C).[108] Since 1985, Stryker (Kalamazoo, MI) has produced porous HDPE (MEDPOR) and HDPE/titanium mesh (MEDPOR TITAN) implants for use in cranio-maxillofacial reconstructive or cosmetic cases.[109] Like other synthetic polymers, there is always a risk of infection and extrusion. The chances of these complications are lessened, however, if the elastic modulus of the biomaterial closely matches that of the native tissue.[110] This is postulated to be due to more evenly distributed mechanical loading across the tissue-implant interface, preventing tension and micromovement that may lead to extrusion. For example, for a hypothetical auricular reconstruction, the modulus of a porous 3D printed HDPE-scaffold was engineered to more closely match that of auricular cartilage when compared to MEDPOR.[81] Additionally, these HDPE-scaffolds have been experimentally loaded and/or coated with bioactive, antimicrobic, and angiogenic substances resulting in dampened inflammatory response and enhanced tissue ingrowth, outperforming their commercial counterparts.[81,111]

3.2.5. Polyetheretherketone.—Polyetheretherketone is a well-described nondegradable, thermoplastic polyaromatic for use in craniofacial reconstruction. PEEK implants are commonly printed via FDM or Selective Laser Sintering.[112] This biomaterial is known for its mechanical strength, modulus similar to cortical bone, and excellent thermal resistance.[73] Unlike the previously mentioned thermoplastic polymers, structurally complex 3D printed PEEK implants can be sterilized by autoclaving without risk of deformation or changes to its biocompatibility.[73,112] It is important to note that a recently published PEEK

Safety Profile by the FDA identified an association between PEEK used in cranioplasty and seizure or exposure of the implant with a moderate quality of evidence.[113] Although it was emphasized that these are complications associated with other biomaterials used for cranioplasty as well.[113] Other craniofacial applications have included correction of zygomatic, mandibular, and orbital rim or floor deformities.[114] Composite scaffolds, such as PEEK/Hydroxyapatite, continue to be evaluated as a candidate for craniofacial defect repair.[74,115] Previous studies have demonstrated increased cellular adhesion, proliferation, and alkaline phosphatase activity with a corresponding decrease in tensile strength.[74,115] In this context, the load-bearing demands of each unique defect environment must be considered.

3.3. Bioceramics.

Bioceramics generally utilized for bone regeneration have included calcium phosphates (CaP), calcium carbonates, calcium sulfates, and bioactive glasses.[116] In contrast to synthetic polymers, bioceramics are inherently osteointegrative, osteoinductive, and osteoconductive.[117] When fabricated as a porous 3D printed scaffold, bioceramics promote a strong tissue-scaffold interface, recruit mesenchymal stem cells (MSCs) to the defect site, and provide bioactive surfaces that facilitate osteogenesis, respectively. In their pure forms, however, they are limited by poor angiogenic properties and slow degradation rates, making these processes occur at an inadequate pace.[117,118] This issue is amplified at the center of large craniofacial defects, which are already under hypoxic conditions. Also, unlike synthetic polymers, bioceramics are mechanically weak and brittle, raising concern for their performative potential within load-bearing defects.[117,119] However, a recent study found that 3D printed β-TCP scaffolds were able to restore critically sized, full-thickness mandibulectomy defects in a rabbit model despite return to normal mastication after implantation.[120] This solidifies their potential to withstand areas of high mechanical stress if they are constructed properly on the microscale. Ongoing strategies to improve the osteogenic and mechanical potential of bioceramic scaffolds have included active component loading, doping with trace elements, bioactive surface coatings, as well as the addition of micro- and nanostructures or alterations to pore size.[117] β-Tricalcium phosphate (β-TCP), a bioactive calcium phosphate, has garnered particular attention within the field of craniomaxillofacial reconstruction given its well-documented safety profile, 6–18-month resorption period, and similar composition to the mineral phase of human bone.[25,84,119] β-TCP resorption kinetics are much more favorable to hydroxyapatite, which exhibits a degradation rate of approximately 1%/year.[121] Direct-Ink-Writing (DIW), or robocasting, with bioactive ceramic colloidal ink followed by sintering allows for customization of a defect-specific scaffold.[25] Sintering effectively improves the scaffold's mechanical strength by densification.[121] Previous studies have suggested optimal outcomes in treating mandibular defects of a rabbit model after scaffold sintering at 1100 °C for 4 h.[120,122] The *in vivo* performance of β-TCP scaffolds has been found to significantly improve with the addition of the FDA-approved pharmaceutical dipyridamole (DIPY). DIPY is an adenosine A_{2A} receptor indirect agonist with a bone regenerative capacity. DIPY-augmented β-TCP scaffolds have been investigated in criticalsized, craniofacial defects within skeletally mature and immature rabbit, ovine, or swine models.[122–130] Shen et al. successfully accelerated the degradation rate of β-TCP to 55%/year (calvarial defect) and 90%/year (alveolar defect)

with the addition of a 1000 μM DIPY coating (Figure 3A,B).[130] This study, as well as other studies performed by this group, found that the β-TCP scaffold was replaced with regenerated, vascularized bone that is similar in its mechanical and histologic properties to native bone.[122–130] If evaluated in a skeletally immature animal model in proximity to a growth suture, the suture remained patent, even past the point of facial growth completion.[126–128,131] This finding is critical as suture obliteration in pediatric patients is a feared complication of β-TCP scaffolds augmented with growth factor, recombinant human bone morphogenic protein (rhBMP-2).[128] Ultimately, replacement of exogenous growth factors, such as rhBMP-2, with regenerative pharmaceuticals, like DIPY, mitigates the deleterious effects associated with their supraphysiological dosing requirements.[132] To summarize the differences between the aforementioned biomaterials, refer to Table 1 for their respective advantages and disadvantages.

4. 3D PRINTING TECHNOLOGIES

According to the ISO and American Society for Testing and Materials (ASTM), there are seven overarching categories of additive manufacturing processes: vat polymerization, material jetting, binder jetting, material extrusion, powder bed fusion, sheet lamination, and directed energy deposition. These 3DP processes differ in their energy sources, suitable printing materials, and methods by which CAD data are used to fabricate individual layers and then solidify and/or fuse them to create the desired design.[133] Several printing techniques may belong within a single category, in which case small nuances distinguish them from one another. Many of these printing techniques have been patented or trademarked by their original developers, adding an additional layer of complexity to the nomenclature. The categories used to 3D print patient-specific anatomical models, surgical guides, or implantable devices in CMF reconstruction broadly include vat photopolymerization, material jetting, material extrusion, and powder bed fusion. Here we seek to discuss the intricacies of each 3D printing technique as they relate to craniofacial surgery.

4.1. Vat Photopolymerization.

The three key components of vat photopolymerization (VPPP) include a light source, a vat, and a light-curable resin.[133,134] For a 3DMD, the resin must be a nontoxic, biocompatible photoactive material.[134] A platform is submersed within a vat, or reservoir, of a liquid resin in its monomer or oligomer form (Figure 4A). A focused curing light irreversibly solidifies the liquid through photopolymerization of these monomers and oligomers.[133] The curing light path follows the segmented layers of the STL model. Once stabilized, the platform is lowered or raised by a constant height to build upon the previous layer until device completion. Layer thickness typically falls between 50 and 100 μm.[135] The printer will also build a removable latticework beneath any overhangs that may require additional support.[133,134] The completed model is withdrawn from the vat, support structures are removed, and the final model is cleansed and then cured within an UV chamber to complete the polymerization process. Techniques within this category are distinguished based upon light curing method, including laser (stereolithography (SLA)), projector (digital

light processing (DLP)), light emitting diodes (LEDs), and oxygen (continuous digital light processing/continuous liquid light processing).[134]

SLA, patented by Charles W. Hull in 1986, is a technique utilized regularly for 3D printing in complex CMF reconstruction. Anatomical models and surgical guides are fabricated using epoxy- or acrylic resins.[134] SLA-printed scaffolds for hard tissue repair can also be developed by using photocurable bioinks. These bioinks are hydrogel-based with or without additional cells or osteoconductive bioceramics (e.g., hydroxyapatite, β-TCP). For example, a scaffold with a perfusable vessel lumen was successfully constructed with a gelatin methacryloyl (GelMA)/nanocrystalline hydroxyapatite bioink for bony defect repair.[136] Recently, SLA-printed bioceramic scaffolds demonstrated robust osteointegration in a rat calvarial model.[137] In this study, HA and β-TCP were mixed with acrylic resin for SLA-printing, followed by thermal cycling of the final construct to remove the resin entirely ahead of implantation. Standard print speed ranges between 10 and 20 mm/h and accuracy is determined by diameter of the laser beam, with small spot sizes allowing for high resolution.[134]

4.2. Material Jetting.

Like vat photopolymerization, material jetting requires a UV light source and a light-curable liquid resin. Unlike VPP, material jetting (MJT) uses thermal force to deliver microdroplets of low-viscosity feedstock, from cartridge to jet head, onto a build platform.[138] Photopolymer materials are extruded in a layered fashion and cured as successive layers are assembled. Layers can be as small as 16 μm in thickness, allowing for intricate geometrical structures with high accuracy.[139,140] Instead of printing a lattice support structure to later be removed as done with VPP processes, all MJT printers require a support material to deposit the build material(s). MultiJet, trademarked by 3DSystems, is a single build material printer supported by a wax.[139] By contrast PolyJet, a MJT system developed by Stratasys, can print multiple build materials supported by a gel.[139] This allows PolyJet printers to create multicolored anatomical models that highlight relevant vasculature and innervation or patient-specific hardware.[141] During postprocessing, MultiJet and PolyJet printers remove support material by melting and waterjet/chemical bath, respectively.[139] PolyJet postprocessing steps are laborious in comparison to those of MultiJet. However, PolyJet is often still the preferred system due to its multimaterial capabilities. A recent study found that compared to surgical guides produced by SLA and digital metal printing (DMP), the PolyJet printer was the most accurate and demonstrated the highest reproducibility, even after 1-month storage of devices.[142] Similarly, the smallest mean difference between 3D printed surgical guide and its CAD model was found when fabricated by a PolyJet printer compared to an SLA or MultiJet system.[143] Bone constructs were also printed with this AM technology. Similar to VPP, biocompatible photopolymers must be used but may be mixed and/or coated with osteoconductive materials, like polydopamine and hydroxyapatite.[144] Although generally, restriction of printable materials to photoreactive polymers is a significant limitation of vat polymerization and material jetting.

4.3. Material Extrusion.

Fused deposition modeling (FDM), trademarked by Stratasys, and fused filament fabrication (FFF) both use thermal material extrusion technology. Within a heated build chamber, FDM dispenses a spool of thermoplastic filament through a heated, pressurized nozzle onto a heated build plate.[133] Like the AM technologies discussed previously, a dissolvable support material is required for material extrusion. This is deposited simultaneously through a second nozzle and removed during postprocessing by hot water or solvent bath.[145] Instead of requiring light-curable resins to be photopolymerized, such as in VPP or MJT, molten layers printed with FDM or FFF simply fuse as they cool. Printable materials include thermoplastic polymers often used for CMF applications such as PEEK, PLA, PLGA, PCL, and bioceramics. It is important to note that FFF is not conducted within a heated build chamber, leading to uneven cooling[146] and inconsistencies in the device's mechanical performance; thus, FDM is preferred if the 3DMD is intended for implantation. FDM has also been found to produce the most dimensionally accurate mandibular models among the material extrusion techniques.[147] That being said, FDM has been employed to fabricate thermoplastic polymer/ceramic composite scaffolds for bone regeneration, anatomical models for resident training, preoperative bending of off-the shelf fixation devices, or to facilitate accurate intraoperative reconstruction, as well as surgical guide fabrication for a range of CMF applications.[148–152]

Direct-ink-writing (DIW) is also a material extrusion AM process but relies entirely on pressurized syringe pumps, without heat, for deposition (Figure 4B).[153] Because of this, emphasis is placed on fine-tuning the ink's rheological properties, such as viscosity, yield stress, and elastic moduli for optimal printability.[153] As it relates to craniofacial surgery, DIW is capable of printing multimaterial structures with thermoplastic polymers (PLA, PGA, PLGA, PCL, PEEK), bioceramics, bioceramic/hydrogel composites, and less frequently titanium when incorporated into a water-based suspension for printing.[121,154,155] A support material may also be necessary for successful DIW and can be removed by dissolution or melting during postprocessing. Additional efforts to facilitate solidification of the 3DMD's final form will vary by material but may include sintering, photocuring, or solvent evaporation.[153]

4.4. Powder Bed Fusion.

Powder bed fusion (PBF) is an AM process that encompasses selective laser sintering (SLS), selective laser melting (SLM), direct metal laser sintering (DMLS), and electron beam melting (EBM). All materials printed by PBF exist as a powder feedstock supplemented with a feeder chamber. Powder is mechanically rolled evenly, and in successive 2D-cross sections, across a neighboring build chamber. Layer thicknesses are reported as 100–120 μm (SLS), 20–100 μm (SLM/DMLS), and 45–150 μm (EBM).[156] The powder is selectively consolidated by melting (SLM, EBM) or sintering (SLS, DMLS). In the case of SLS, SLM, and DMLS the heat source enabling solidification is a high-power laser and, in EBM, an electron beam. The surrounding, unconsolidated powder serves as a support to the 3DMD as it is built. Although, additional support may be warranted for structures with complex geometries. One advantage of PBF, unlike VPP, is unused powder can be recycled for future build cycles; however this should be done cautiously as studies have

reported alterations to several mechanical properties of the final device.[157] In respect to CMF applications, EBM, SLM, and DMLS can print powdered titanium or TiAl6 V4 ELI, whereas SLS prints powdered thermoplastic polymers (e.g., PE, PEEK, PLA, PCL) or ceramics.[158] Postprocessing involves compressed air to remove any unconsolidated powder, as well as numerous grinding and/or polishing procedures to adjust surface roughness.[159] Overall, PBF AM processes are great options for printing patient-specific surgical plates, fixation devices, or scaffolds for CMF bone repair.[160–162]

5. STERILIZATION TECHNIQUES

After printing, the devices must be adequately sterilized without compromising their final form. To be FDA-cleared for intraoperative use, all 3DMD require validation of a certain sterility assurance level (SAL).[163] The SAL is defined as the expected probability of a living microorganism following sterilization.[164] FDA requires an SAL < 10^{-3} for any device touching skin and SAL < 10^{-6} for an implantable device. Additionally, implantable devices necessitate pyrogenicity testing to rule out presence of Gram-negative endotoxins or material-mediated pyrogens that may cause a febrile reaction in the patient.[165]

Sterilization techniques are distinguished by class on the basis of their known level of efficacy. Established Category A have been deemed safe and effective, with the most literature in support of their efficacy.[165] This class encompasses dry heat, ethyl oxide (EO) in a fixed chamber, steam (e.g., autoclave), and radiation (e.g., gamma or electron beam) sterilization.[165] Sterilizers within Established Category B do not have any FDA-recognized consensus standards but do have an established place in the literature.[165] Established Category B includes hydrogen peroxide, ozone, and EO in a flexible bag system.[165] The final category is known as Novel Sterilization Methods and includes vaporized peracetic acid, high intensity light, micro-wave radiation, sound waves, and ultraviolet light.[165] These methods have not been FDA-reviewed nor determined to adequately sterilize products, however, may become viable sterilization options in the future.[165]

The mechanical and physical properties of the materials within a 3DMD determine the safest method for sterilization. Due to its high melting point and Young's modulus, a 3DMD made from titanium is sterilizable by irradiation or autoclaving without risk of deformation.[166] Similarly, PEEK 3DMD can be sterilized by autoclave without significant changes to its dimensional accuracy.[73,107,167] By contrast, PMMA devices should not be sterilized by autoclave as conflicting data exists regarding structural compromise.[107,168] The remaining thermoplastic materials, PLA, PGA, PLGA, PE and PCL, are not survivable by autoclave, dry heat, or EO sterilization without altering their final structure or mechanical properties.[169,170] H_2O_2 plasma vapor sterilization, ethanol, and electron beam irradiation have been found to be the safest sterilization techniques for PGA/PLGA and polycaprolactone.[169,171] Steam sterilization by autoclave (121 °C for 40 min) has been found to alter the physiochemical properties and pH of porous bioceramics with a concern that this would affect their osteoinductivity/osteoconductivity *in vivo*.[172]

6. ECONOMICS

Since the approval of 3D printing-related Current Procedural Terminology (CPT) codes for anatomic models and surgical guides in 2018, interest to incorporate 3DMD in routine surgical care has grown exponentially.[173] By 2028, the 3DMD market is projected to be a $6.9B industry with an annual growth rate 17.1%.[174] Establishment of a POC 3DP facility has enormous benefits to both patients and surgeons within the private and academic sectors. As it stands, extended manufacturing and transport times due to distant third-party manufacturers bottleneck widespread use of the technology. For example, 3DMD cannot be used in acute CMF trauma cases, although if available it would alleviate many of the challenges associated with reconstruction of extensive facial traumas.[4] Additionally, the tendency to incorporate biologics (e.g., stem cells) into 3D printed scaffolds is not conducive to transport across great distances. Thus, HCFs can differentiate themselves by having such capabilities in-house. As of 2019, there were 113 hospitals in the United States with centralized 3D printing capabilities.[175] An HCF considering the establishment of their own POC facility must first consider the cost of all the required materials and equipment needed for the 3DP workflow.

The first requirement is a 3D printer and compatible segmentation software. The 3D printer itself has the largest upfront cost. Depending on the type, processing speed, manufacturer, and desired printable materials, cost ranges widely with a mean of approximately $100,000.[35,176] Several of the more inexpensive options with many potential CMF applications are material jetting, material extrusion, and stereolithography printers.[35,140,177] It is important to emphasize that only a select number of printers currently on the market are FDA-cleared for 3DMD fabrication.[35] Options that have been coined as low cost, such as an inexpensive material extrusion printer, have not yet been validated by the FDA, despite similar clinical performance.[178,179] The price of segmentation software typically requires a quote, as they depend on the size and output of the 3D printing system. Some software are accompanied by their own biomedical engineers available to collaborate directly with surgeons. Their labor fees in addition to any other individuals necessary to oversee and maintain the equipment must also be accounted for in the overall cost of a POC 3D printing facility.

An additional cost to consider is the required printing materials. Their prices fluctuate heavily based on supply and demand in a commodity-like market. For example, as of June 2023, polylactic acid was trading at $2.66/kg.[180] By contrast, PEEK is valued at hundreds of dollars per kilogram.[181] A 1-year trend in cost per kilogram of common 3D printed materials can be seen in Figure 5A and B with the volatility and percent change per month of their respective costs over the past year depicted in Table 2.[180,182–184] While these prices are seemingly inexpensive compared to the larger upfront costs discussed earlier, this would be a recurring expense for the HCF.

The average cost for an anatomical model produced by industry was $2467 with some reported to be as high as $6000.[150,185,186] Conversely, a recent study noted that the average cost for 3D printed anatomical models produced in-house was $2180.[185] Despite this initial cost, 3D printed anatomical model and surgical guides are estimated to save hospitals $5172

and $1918, respectively, due to reductions in operative time per case.[173] That being said, it is predicted that an HCF must print a volume of 63 models or guides annually to cover the costs of having the 3DP system itself.[173] Because of the extensive FDA-clearance process required for implantable 3DMD, there are few data reported currently on costs saved, if any, because of their use.

7. CLINICAL APPLICATIONS OF 3DMD IN CMF SURGERY

Considering both the barriers and benefits associated with 3DMD discussed thus far, it is understandable that anatomical models, surgical guides, and implants are slowly, yet excitedly, making their way into operating rooms for CMF application. Barriers have centered on the establishment of FDA-regulatory oversight and the expenses associated with this new and ever-developing technology. Cumulatively, the benefits of 3D printed anatomical models and surgical guides are theorized to include improved surgical accuracy, decreased operative time, and fewer complications. Additionally, *in vitro* and *in vivo* studies of patient-specific implants have established their potential to restore critical-sized defects in both load-bearing and nonload-bearing regions of the craniofacial region. However, surgeon familiarity, imaging quality, material, production equipment, and patient anatomy are all confounding variables that may hinder 3DMDs' clinical performance. This section serves as a discussion of the most recent and representative clinical cases in craniomaxillofacial surgery that have utilized 3D printed models, guides, and implants produced by additive manufacturing processes.

7.1. Anatomical Models.

Anatomical models allow surgeons to tangibly visualize patient anatomy, developing a clearer, more efficient surgical plan for complex cranio-maxillofacial reconstructions. Anatomical model development is the product of a process known as virtual surgical planning (VSP). A digital simulation of the surgical intervention is generated from patient high resolution CT data collaboratively among the CMF reconstructive team and biomedical engineer. A study that 3D printed an auricular model for a microtia case highlights the dramatic difference that can exist between material cost alone and labor fees associated with model design (i.e., $1 vs $500, respectively).[150] This data is then used to print the patient-specific model in addition to surgical guides or implants when warranted. The broad scope of anatomical model applications in oncologic, traumatic, and congenital CMF reconstruction is described in Table 3. Within this subset of representative cases, SLA[187–192] and FDM[150,190,193,194] were the most commonly employed AM techniques. Models were studied both preoperatively and intraoperatively for surgery simulation and resident training, patient education, situating hardware and/or implant placement, and bending off-the-shelf fixation devices to anatomical contours. Reported benefits broadly included decreased operative time, decreased need for surgical estimations and thus higher accuracy, and improved patient education and modulation of expectations.

7.2. Surgical Guides.

The primary function of 3D printed surgical guides is to serve as templates to facilitate safe and accurate bone cutting or to properly position the device placement. Table 4 is a

representative summary of the various recent applications of surgical guides in CMF surgery. Although traditionally thought to be used strictly intraoperatively, surgical guides were also used preoperatively to perform mock surgeries on patient-specific anatomical models.[195] Very few identified studies disclosed the AM technique, but of those that did, SLA and FDM were the most common. Material of choice were various polymers, and in only one study was a titanium surgical guide made.[31] In this case the titanium surgical guide was preferred, although much more expensive, to avoid risk of polymer deterioration and to guarantee guide stability and rigidity.[31] Other parameters including cost, time to manufacture, and sterilization method were scarcely mentioned in the existing literature. Overarching benefits included decreased operative time, prevention of injury to critical nearby structures, accurate and symmetrical cutting and implant placement, and overall improved patient outcomes.[196] One caution that was raised in the case of oncologic reconstruction was the risk of tumor growth between the time of VSP and the day of surgery. In this case, it was encouraged that cutting guides be developed with a slight overestimation of defect size.[197]

7.3. Implants.

To date, 3D printed implants have been utilized largely in cranioplasties and nasal, orbital, maxillary, and mandibular reconstruction (Table 5). Titanium and thermoplastic polymers, predominantly PEEK, were the materials of choice for orbital, nasal, maxillary, and mandibular reconstruction.[114,198–208] In addition to these materials, the use of 3D printed bioceramics has also been attempted in cranioplasties.[209–213] Of note, many of these studies were performed outside of the United States and largely in adults with few exceptions of pediatric patients. Implant cost, time to manufacture, and sterilization methods were rarely reported, despite being some of the most widely discussed limitations of 3DMD. Commonly reported benefits mentioned were physician and patient aesthetic satisfaction, improved implant fit to anatomical contours, and reduced operative time. However, 3 of the 17 identified studies reported development of an implant with an improper fit due to errors with the initial CT scan or conversion to CAD.[200–202] It must be emphasized that each transition step within the 3D printing process introduces an opportunity for inaccuracy. Imaging quality of CT- and MRI-data have been reported to modulate the mean absolute error between virtual 3D model and final printed product.[35] Furthermore, the use of CAD software to develop a 3D printer compatible file has also been shown to compromise the integrity of the original scan.[35] As a part of their quality system regulations, FDA-approved software platforms verify preservation of original scan data.[35] It is imperative that HCFs purchase FDA-cleared software and compatible printers when planning to establish their own POC 3D printing facility. Future clinical studies should aim to report as much information as possible regarding the various stages of their unique 3D printing workflow to facilitate reproducibility and build a foundational clinical database.

8. FUTURE DIRECTIONS

8.1. Automatization of 3D Printed Implant Design.

With the focus of HCFs and the U.S. FDA alike on the development of hospital-operated 3DP facilities, researchers have begun to investigate the automatization of the user-dependent aspects of the 3DP workflow. More specifically, the challenge of accurate 3DMD

formulation lies within the conversion from original scan data to DICOM, and finally to a 3D printable file. This process is both timely and technically complex, posing a challenge to inexperienced users. To combat this issue, Li et al. developed a database of CT-based, healthy cranial scans injected with randomly generated artificial defects.[224] The goal is to train deep learning algorithms, by way of data sets like these, to perform automatic defect reconstruction and implant generation.[224] This would save time, reduce labor expenses, and improve implant design accuracy by eliminating risk of human error, which is a frequently reported cause of improper fit of 3D printed implants.[200–202] The deep learning algorithm can be refined to generate implant designs for real CMF defects more accurately if other researchers contribute their own scan data to the database.[224]

8.2. 3DMD + Augmented Reality.

With the latest advancements in augmented reality (AR) technology, commercial AR platforms have become available for surgical use. AR allows the user to virtually visualize an overlay of critical patient anatomy (e.g., arterial supply, innervation, musculature) that may not be visible in reality.[225] The virtual, holographic projections are generated from patient CT/MRI data and registered in that specific surgical field. AR can be combined with 3D printing technology for resident training, preoperative planning, or intraoperatively to accurately position surgical guides and subsequent fixation devices. Thus, far, this technology has been successfully applied in craniosynostosis, face transplantation, mandibular and auricular reconstruction, as well as for patient-specific facial artery mapping.[214,225–229] With adequate training, reported outcomes have included improved accuracy, minimization of operative injury, reduced costs, and shortened intraoperative time.[225]

8.3. *In Situ* Bioprinting.

In situ bioprinting is a rapidly advancing form of 3D bioprinting in which biomaterials/bioinks are used print acellular/cell-laden constructs, respectively, directly into the desired defect site.[230] Subtypes include bedside mounted (e.g., traditional *in situ* bioprinter, robotic-arm assisted bioprinter) and hand-held (e.g., ionically activated, light activated) printers; both of which can be used in a sterile surgical suite. *In situ* bioprinting research for CMF repair remains in its preclinical stages, with critical-sized, murine calvaria defects.[231–233] For example, Kérourédan et al. printed endothelial cell-based microvascular networks in defects prefilled with collagen, MSCs, and VEGF.[231] This experimental group exhibited improved vascularization and bone regeneration compared with scaffolds randomly seeded with endothelial cells and negative controls. Relative to *ex vivo* bioprinting (i.e., premade constructs), clinical application of *in situ* bioprinting would eliminate many challenges associated with the production of 3DMD with biologic components. More specifically, printing directly onto the patient would minimize contamination risk and implantation delays associated with *ex vivo* manufacturing and transportation.[231]

8.4. 4D Printing.

4D printing is defined by the ability of 3D printed structures to temporarily transform and reform to an original shape when cued by an external stimulus. Stimuli can include but are not limited to temperature, water or solvents, magnetism, and ultraviolet light.[234]

Shape transformations such as folding, curling, twisting, and linear expansion have all been achieved. This technology has the potential to optimize bone defect repair with 3D printed scaffolds. For example, Senatov et al. 3D printed a PLA/15 wt % HA porous scaffold by fused filament fabrication with heat-sensitive shape memory.[235] Clinically, scaffolds can be surgically inserted in their compact, deformed shape and upon shape-memory activation, expand to precisely fit the bone defect.[235,236] As it stands, a limitation of 4D printing is identifying materials that are responsive to stimuli that are benign to humans. For example, heat-sensitive shape memory is only feasible if it is within the range of human body temperature.[234] Soybean oil epoxidized acrylate fabricated scaffolds have recently been discovered to be capable of such transformations and have even demonstrated promising osteoconductive potential.[234] This technology has also been harnessed to create 3DMD capable of shape change with tissue growth, with enormous implications for pediatric cranio-maxillofacial bone repair as the scaffold could expand with skeletal development.[237]

9. CONCLUSION

3D printing technology within the field of craniomaxillofacial surgery has grown exponentially in recent decades. Possible applications have proven to touch every aspect of the field with an overarching ability to improve functional and aesthetic outcomes as well as reduce the operative time and postoperative complications. Researchers continue to push the envelope with the capabilities of 3DMD, including shape memory devices. This has the potential to disrupt current standard-of-care for pediatric craniofacial patients. Craniofacial surgeons excitedly introduce anatomic models, surgical guides, and implantable devices into their operating rooms, proving or disproving their benefits on a case-by-case basis and furthering the research as a result. Meanwhile, the FDA is working diligently with stakeholders to discuss feasible ways to provide this care safely and accessibly to patients at the point-of-care. As discussed, 3DMD has the potential to become the new standard within CMF surgery. In order to prepare for 3DMD finding its eventual commonplace, it is imperative that this technology continue to be better understood, discussed, and refined for all of its applications within craniomaxillofacial surgery.

Funding

Some of the work referenced/discussed in this review was supported by DoD (W81XWH-16-1-0772 MPI-Rodriguez, Coelho); NIH-NIAMS (R01AR068593—MPI: Paulo G. Coelho and Bruce N. Cronstein); NIH-NICHD (R21HD090664—MPI: Paulo G. Coelho, Bruce N. Cronstein, and Roberto L. Flores; R33HD090664—MPI: Paulo G. Coelho, Bruce N. Cronstein, Roberto L. Flores, and Lukasz Witek); and the Osteo Science Foundation (Peter Geistlich Research Award MPI: Simon Young, F. Kurtis Kasper, Paulo G. Coelho, and Lukasz Witek

REFERENCES

(1). Bous RM; Hazen RA; Baus I; Palomo JM; Kumar A; Valiathan M Psychosocial Adjustments Among Adolescents With Craniofacial Conditions and the Influence of Social Factors: A Multi-Informant Study. Cleft Palate Craniofac J. 2020, 57 (5), 624–636. [PubMed: 31769310]

(2). Johns AL; Stock NM; Costa B; Billaud Feragen K; Crerand CE Psychosocial and Health-Related Experiences of Individuals With Microtia and Craniofacial Microsomia and Their Families: Narrative Review Over 2 Decades. Cleft Palate Craniofac J. 2023, 60, 1090. [PubMed: 35382590]

(3). Roberts RM; Shute R Children's experience of living with a craniofacial condition: perspectives of children and parents. Clin Child Psychol Psychiatry 2011, 16 (3), 317–34. [PubMed: 20650974]

(4). Salinas CA; Morris JM; Sharaf BA Craniomaxillofacial Trauma: The Past, Present and the Future. J. Craniofac Surg 2023, 34, 1427. [PubMed: 37072888]

(5). Koons GL; Diba M; Mikos AG Materials design for bonetissue engineering. Nature Reviews Materials 2020, 5 (8), 584–603.

(6). Gaihre B; Uswatta S; Jayasuriya AC Reconstruction of Craniomaxillofacial Bone Defects Using Tissue-Engineering Strategies with Injectable and Non-Injectable Scaffolds. J. Funct Biomater 2017, 8 (4), 49. [PubMed: 29156629]

(7). Neovius E; Engstrand T Craniofacial reconstruction with bone and biomaterials: review over the last 11 years. J. Plast Reconstr Aesthet Surg 2010, 63 (10), 1615–23. [PubMed: 19577527]

(8). Nguyen PD; Khechoyan DY; Phillips JH; Forrest CR Custom CAD/CAM implants for complex craniofacial reconstruction in children: Our experience based on 136 cases. J. Plast Reconstr Aesthet Surg 2018, 71 (11), 1609–1617. [PubMed: 30220563]

(9). Emara A; Shah R Recent update on craniofacial tissue engineering. J. Tissue Eng 2021, 12, 204173142110037.

(10). Amini AR; Laurencin CT; Nukavarapu SP Bone tissue engineering: recent advances and challenges. Crit Rev. Biomed Eng 2012, 40 (5), 363–408. [PubMed: 23339648]

(11). Asti A; Gioglio L Natural and synthetic biodegradable polymers: different scaffolds for cell expansion and tissue formation. Int. J. Artif Organs 2014, 37 (3), 187–205. [PubMed: 24744164]

(12). Rindone AN; Nyberg E; Grayson WL 3D-Printing Composite Polycaprolactone-Decellularized Bone Matrix Scaffolds for Bone Tissue Engineering Applications. Methods Mol. Biol 2017, 1577, 209–226.

(13). Yang WF; Choi WS; Leung YY; Curtin JP; Du R; Zhang CY; Chen XS; Su YX Three-dimensional printing of patient-specific surgical plates in head and neck reconstruction: A prospective pilot study. Oral Oncol 2018, 78, 31–36. [PubMed: 29496055]

(14). Wang CF; Yu Y; Bai W; Han JM; Zhang WB; Peng X Mechanical properties of three-dimensionally printed titanium plates used in jaw reconstruction: preliminary study. Int. J. Oral Maxillofac Surg 2022, 51 (6), 754–761. [PubMed: 34629260]

(15). Tantisatirapong S; Khunakornpattanakarn S; Suesatsakul T; Boonpratatong A; Benjamin I; Tongmeesee S; Kangkorn T; Chanwimalueang T The simplified tailor-made workflows for a 3D slicer-based craniofacial implant design. Sci. Rep 2023, 13 (1), 2850. [PubMed: 36801943]

(16). Yang WF; Zhang CY; Choi WS; Zhu WY; Li DTS; Chen XS; Du R; Su YX A novel 'surgeon-dominated' approach to the design of 3D-printed patient-specific surgical plates in mandibular reconstruction: a proof-of-concept study. Int. J. Oral Maxillofac Surg 2020, 49 (1), 13–21. [PubMed: 31230767]

(17). Martola M; Lindqvist C; Hanninen H; Al-Sukhun J Fracture of titanium plates used for mandibular reconstruction following ablative tumor surgery. J. Biomed Mater. Res. B Appl. Biomater 2007, 80 (2), 345–52. [PubMed: 16850467]

(18). Liu SP; Cai ZG; Zhang J; Zhang JG; Zhang Y [Plate related complication after mandibular reconstruction]. Zhonghua Kou Qiang Yi Xue Za Zhi 2013, 48 (10), 586–90. [PubMed: 24438564]

(19). Hauk V Structural and residual stress analysis by nondestructive methods: Evaluation-Application-Assessment; Elsevier, 1997; p v.

(20). Parthasarathy J 3D modeling, custom implants and its future perspectives in craniofacial surgery. Ann. Maxillofac Surg 2014, 4 (1), 9–18. [PubMed: 24987592]

(21). Khorsandi D; Fahimipour A; Abasian P; Saber SS; Seyedi M; Ghanavati S; Ahmad A; De Stephanis AA; Taghavinezhaddilami F; Leonova A; Mohammadinejad R; Shabani M; Mazzolai B; Mattoli V; Tay FR; Makvandi P 3D and 4D printing in dentistry and maxillofacial surgery: Printing techniques, materials, and applications. Acta Biomater 2021, 122, 26–49. [PubMed: 33359299]

(22). Zhu W; Ma X; Gou M; Mei D; Zhang K; Chen S 3D printing of functional biomaterials for tissue engineering. Curr. Opin Biotechnol 2016, 40, 103–112. [PubMed: 27043763]

(23). Do AV; Khorsand B; Geary SM; Salem AK 3D Printing of Scaffolds for Tissue Regeneration Applications. Adv. Healthc Mater 2015, 4 (12), 1742–62. [PubMed: 26097108]

(24). Ren B; Wan Y; Liu C; Wang H; Yu M; Zhang X; Huang Y Improved osseointegration of 3D printed Ti-6Al-4V implant with a hierarchical micro/nano surface topography: An in vitro and in vivo study. Mater. Sci. Eng. C Mater. Biol. Appl 2021, 118, 111505. [PubMed: 33255064]

(25). Witek L; Nayak VV; Runyan CM; Tovar N; Elhage S; Melville JC; Young S; Kim DH; Cronstein BN; Flores RL Tissue Engineering Strategies for Craniomaxillofacial Surgery: Current Trends in 3D-Printed Bioactive Ceramic Scaffolds. Innovative Bioceramics in Translational Medicine II: Surgical Applications 2022, 18, 55–74.

(26). Fahimipour F; Rasoulianboroujeni M; Dashtimoghadam E; Khoshroo K; Tahriri M; Bastami F; Lobner D; Tayebi L 3D printed TCP-based scaffold incorporating VEGF-loaded PLGA microspheres for craniofacial tissue engineering. Dent Mater. 2017, 33 (11), 1205–1216. [PubMed: 28882369]

(27). Qian Y; Zhou X; Zhang F; Diekwisch TGH; Luan X; Yang J Triple PLGA/PCL Scaffold Modification Including Silver Impregnation, Collagen Coating, and Electrospinning Significantly Improve Biocompatibility, Antimicrobial, and Osteogenic Properties for Orofacial Tissue Regeneration. ACS Appl. Mater. Interfaces 2019, 11 (41), 37381–37396. [PubMed: 31517483]

(28). Tel A; Costa F; Sembronio S; Lazzarotto A; Robiony M All-in-one surgical guide: A new method for cranial vault resection and reconstruction. J. Craniomaxillofac Surg 2018, 46 (6), 967–973. [PubMed: 29716817]

(29). Crist TE; Mathew PJ; Plotsker EL; Sevilla AC; Thaller SR Biomaterials in Craniomaxillofacial Reconstruction: Past, Present, and Future. J. Craniofac Surg 2021, 32 (2), 535–540. [PubMed: 33704977]

(30). Jacobs CA; Lin AY A New Classification of Three-Dimensional Printing Technologies: Systematic Review of Three-Dimensional Printing for Patient-Specific Craniomaxillofacial Surgery. Plast Reconstr Surg 2017, 139 (5), 1211–1220. [PubMed: 28445375]

(31). Kim SH; Kim AH; Choi YJ; Jung YS; Kim JY Personalized 3D-printed Titanium Cutting Guide and Prefabricated Osteosynthesis Plate for Mandibular Step Osteotomy to Treat Severe Mandibular Prognathism. J. Craniofac Surg 2022, 33 (7), 2247–2251. [PubMed: 35882014]

(32). Breakthrough Devices Program; U.S. FDA, 2023. https://www.fda.gov/medical-devices/how-study-and-market-your-device/breakthrough-devices-program#s1 (accessed 07-10-2023).

(33). Technical Considerations for Additive Manufactured Medical Devices; U.S. FDA, 2017; pp 1–31.

(34). 21, C.F.R. § 820.1, Code of Federal Regulations; National Archives, 2023. https://www.ecfr.gov/current/title-21/chapter-I/subchapter-H/part-820 (accessed 07-19-2023).

(35). Paxton NC Navigating the intersection of 3D printing, software regulation and quality control for point-of-care manufacturing of personalized anatomical models. 3D Print Med. 2023, 9 (1), 9. [PubMed: 37024730]

(36). Piotrowski SL; Wilson L; Dharmaraj N; Hamze A; Clark A; Tailor R; Hill LR; Lai S; Kasper FK; Young S Development and Characterization of a Rabbit Model of Compromised Maxillofacial Wound Healing. Tissue Eng. Part C. Methods 2019, 25 (3), 160–167. [PubMed: 30747042]

(37). Classify Your Medical Device; U.S. FDA, 2023. https://www.fda.gov/medical-devices/overview-device-regulation/classify-your-medical-device (accessed 07-19-2023).

(38). The 510(k) Program: Evaluating Substantial Equivalence in Premarket Notifications [510(k)]; U.S. FDA, 2014; pp 1–39.

(39). Ricles LM; Coburn JC; Di Prima M; Oh SS Regulating 3D-printed medical products. Sci. Transl Med 2018, 10 (461). DOI: 10.1126/scitranslmed.aan6521.

(40). Factors to Consider When Making Benefit-Risk Determinations in Medical Device Premarket Approval and De Novo Classifications; U.S. FDA, 2019; pp 1–75.

(41). 510(k) Premarket Notification; U.S. FDA, 2015. https://www.accessdata.fda.gov/scripts/cdrh/cfdocs/cfPMN/pmn.cfm?ID=K151692 (accessed 10-24-2023).

(42). BioArchitects Patient Specific Cranial/Craniofacial Plate; Bio-Architects, 2023.

(43). BioArchitects Completely Customized Titanium Implants; Bio-Architects, 2023. https://www.bioarchitects.com/prostheses (accessed 10-24-2023).

(44). Medical Device Databases; U.S. FDA, 2023. https://www.fda.gov/medical-devices/device-advice-comprehensive-regulatory-assistance/medical-device-databases (accessed 10-24-2023).

(45). Discussion Paper: 3D Printing Medical Devices at the Point of Care; U.S. FDA, 2021; pp 1–19.

(46). Kirby B; Kenkel JM; Zhang AY; Amirlak B; Suszynski TM Three-dimensional (3D) synthetic printing for the manufacture of non-biodegradable models, tools and implants used in surgery: a review of current methods. J. Med. Eng. Technol 2021, 45 (1), 14–21. [PubMed: 33215944]

(47). Hatamleh MM Preparation and In Vitro Analysis of Craniofacial Titanium Implants Surfaces Produced by Additive 3D Printing and Conventional Manufacturing. Craniomaxillofac Trauma Reconstr 2021, 14 (3), 224–230. [PubMed: 34471478]

(48). Trindade R; Albrektsson T; Galli S; Prgomet Z; Tengvall P; Wennerberg A Bone Immune Response to Materials, Part I: Titanium, PEEK and Copper in Comparison to Sham at 10 Days in Rabbit Tibia. J. Clin Med 2018, 7 (12), 526. [PubMed: 30544551]

(49). Trindade R; Albrektsson T; Galli S; Prgomet Z; Tengvall P; Wennerberg A Bone Immune Response to Materials, Part II: Copper and Polyetheretherketone (PEEK) Compared to Titanium at 10 and 28 Days in Rabbit Tibia. J. Clin Med 2019, 8 (6), 814. [PubMed: 31181635]

(50). Trindade R; Albrektsson T; Tengvall P; Wennerberg A Foreign Body Reaction to Biomaterials: On Mechanisms for Buildup and Breakdown of Osseointegration. Clin Implant Dent Relat Res. 2016, 18 (1), 192–203. [PubMed: 25257971]

(51). Niinomi M; Nakai M Titanium-Based Biomaterials for Preventing Stress Shielding between Implant Devices and Bone. Int. J. Biomater 2011, 2011, 836587. [PubMed: 21765831]

(52). Chen Q; Thouas GA Metallic implant biomaterials. Materials Science and Engineering: R: Reports 2015, 87, 1–57.

(53). Choi MG; Koh HS; Kluess D; O'Connor D; Mathur A; Truskey GA; Rubin J; Zhou DX; Sung KL Effects of titanium particle size on osteoblast functions in vitro and in vivo. Proc. Natl. Acad. Sci. U. S. A 2005, 102 (12), 4578–83. [PubMed: 15755807]

(54). Saldana L; Vilaboa N Effects of micrometric titanium particles on osteoblast attachment and cytoskeleton architecture. Acta Biomater 2010, 6 (4), 1649–60. [PubMed: 19861182]

(55). Smeets R; Schollchen M; Gauer T; Aarabi G; Assaf AT; Rendenbach C; Beck-Broichsitter B; Semmusch J; Sedlacik J; Heiland M; Fiehler J; Siemonsen S Artefacts in multimodal imaging of titanium, zirconium and binary titanium-zirconium alloy dental implants: an in vitro study. Dentomaxillofac Radiol 2017, 46 (2), 20160267. [PubMed: 27910719]

(56). Kormi E; Mannisto V; Lusila N; Naukkarinen H; Suojanen J Accuracy of Patient-Specific Meshes as a Reconstruction of Orbital Floor Blow-Out Fractures. J. Craniofac Surg 2021, 32 (2), No. e116–e119. [PubMed: 33705044]

(57). Demirturk Kocasarac H; Ustaoglu G; Bayrak S; Katkar R; Geha H; Deahl ST 2nd; Mealey BL; Danaci M; Noujeim M Evaluation of artifacts generated by titanium, zirconium, and titanium-zirconium alloy dental implants on MRI, CT, and CBCT images: A phantom study. Oral Surg Oral Med. Oral Pathol Oral Radiol 2019, 127 (6), 535–544. [PubMed: 30879914]

(58). Wellenberg RHH; Hakvoort ET; Slump CH; Boomsma MF; Maas M; Streekstra GJ Metal artifact reduction techniques in musculoskeletal CT-imaging. Eur. J. Radiol 2018, 107, 60–69. [PubMed: 30292274]

(59). Hargreaves BA; Worters PW; Pauly KB; Pauly JM; Koch KM; Gold GE Metal-induced artifacts in MRI. AJR Am. J. Roentgenol 2011, 197 (3), 547–55. [PubMed: 21862795]

(60). Campbell CA; Lin KY Complications of rigid internal fixation. Craniomaxillofac Trauma Reconstr 2009, 2 (1), 41–7. [PubMed: 22110796]

(61). Berryhill WE; Rimell FL; Ness J; Marentette L; Haines SJ Fate of rigid fixation in pediatric craniofacial surgery. Otolaryngol Head Neck Surg 1999, 121 (3), 269–73. [PubMed: 10471869]

(62). Alasfar RH; Ahzi S; Barth N; Kochkodan V; Khraisheh M; Koc M A Review on the Modeling of the Elastic Modulus and Yield Stress of Polymers and Polymer Nanocomposites: Effect of Temperature, Loading Rate and Porosity. Polymers (Basel) 2022, 14 (3), 360. [PubMed: 35160350]

(63). Jose G; Shalumon KT; Liao HT; Kuo CY; Chen JP Preparation and Characterization of Surface Heat Sintered Nano-hydroxyapatite and Nanowhitlockite Embedded Poly (Lactic-co-glycolic

Acid) Microsphere Bone Graft Scaffolds: In Vitro and in Vivo Studies. Int. J. Mol. Sci 2020, 21 (2), 528. [PubMed: 31947689]

(64). Bell RB; Kindsfater CS The use of biodegradable plates and screws to stabilize facial fractures. J. Oral Maxillofac Surg 2006, 64 (1), 31–9. [PubMed: 16360854]

(65). Mbogori M; Vaish A; Vaishya R; Haleem A; Javaid M Poly-Ether-Ether-Ketone (PEEK) in orthopaedic practice-A current concept review. Journal of Orthopaedic Reports 2022, I (I), 3–7.

(66). Janickova M; Statelova D; Mikuskova K; Jesenak M; Malachovsky I Biodegradable versus titanium plates and screws for paediatric facial skeleton fractures. Bratisl Lek Listy 2018, 119 (9), 554–559. [PubMed: 30226065]

(67). Liao C; Li Y; Tjong SC Polyetheretherketone and Its Composites for Bone Replacement and Regeneration. Polymers (Basel) 2020, 12 (12), 2858. [PubMed: 33260490]

(68). Prado FB; Freire AR; Claudia Rossi A; Ledogar JA; Smith AL; Dechow PC; Strait DS; Voigt T; Ross CF Review of In Vivo Bone Strain Studies and Finite Element Models of the Zygomatic Complex in Humans and Nonhuman Primates: Implications for Clinical Research and Practice. Anat Rec (Hoboken) 2016, 299 (12), 1753–1778. [PubMed: 27870351]

(69). Joshi MK; Lee S; Tiwari AP; Maharjan B; Poudel SB; Park CH; Kim CS Integrated design and fabrication strategies for biomechanically and biologically functional PLA/beta-TCP nanofiber reinforced GelMA scaffold for tissue engineering applications. Int. J. Biol. Macromol 2020, 164, 976–985. [PubMed: 32710964]

(70). Shin DY; Kang MH; Kang IG; Kim HE; Jeong SH In vitro and in vivo evaluation of polylactic acid-based composite with tricalcium phosphate microsphere for enhanced biodegradability and osseointegration. J. Biomater Appl 2018, 32 (10), 1360–1370. [PubMed: 29544380]

(71). Dewey MJ; Milner DJ; Weisgerber D; Flanagan CL; Rubessa M; Lotti S; Polkoff KM; Crotts S; Hollister SJ; Wheeler MB; Harley BAC Repair of critical-size porcine craniofacial bone defects using a collagen-polycaprolactone composite biomaterial. Biofabrication 2022, 14 (1), 014102.

(72). Kao CT; Lin CC; Chen YW; Yeh CH; Fang HY; Shie MY Poly(dopamine) coating of 3D printed poly(lactic acid) scaffolds for bone tissue engineering. Mater. Sci. Eng. C Mater. Biol. Appl 2015, 56, 165–73. [PubMed: 26249577]

(73). Roskies M; Jordan JO; Fang D; Abdallah MN; Hier MP; Mlynarek A; Tamimi F; Tran SD Improving PEEK bioactivity for craniofacial reconstruction using a 3D printed scaffold embedded with mesenchymal stem cells. J. Biomater Appl 2016, 31 (1), 132–9. [PubMed: 26980549]

(74). Manzoor F; Golbang A; Jindal S; Dixon D; McIlhagger A; Harkin-Jones E; Crawford D; Mancuso E 3D printed PEEK/HA composites for bone tissue engineering applications: Effect of material formulation on mechanical performance and bioactive potential. J. Mech Behav Biomed Mater 2021, 121, 104601. [PubMed: 34077906]

(75). Nyberg E; Rindone A; Dorafshar A; Grayson WL Comparison of 3D-Printed Poly-varepsilon-Caprolactone Scaffolds Functionalized with Tricalcium Phosphate, Hydroxyapatite, Bio-Oss, or Decellularized Bone Matrix. Tissue Eng. Part A 2017, 23 (11–12), 503–514. [PubMed: 28027692]

(76). Nyberg E; Farris A; O'Sullivan A; Rodriguez R; Grayson W Comparison of Stromal Vascular Fraction and Passaged Adipose-Derived Stromal/Stem Cells as Point-of-Care Agents for Bone Regeneration. Tissue Eng. Part A 2019, 25 (21–22), 1459–1469. [PubMed: 30734661]

(77). On SW; Cho SW; Byun SH; Yang BE Bioabsorbable Osteofixation Materials for Maxillofacial Bone Surgery: A Review on Polymers and Magnesium-Based Materials. Biomedicines 2020, 8 (9), 300. [PubMed: 32825692]

(78). Zhang J; Tian W; Chen J; Yu J; Zhang J; Chen J The application of polyetheretherketone (PEEK) implants in cranioplasty. Brain Res. Bull 2019, 153, 143–149. [PubMed: 31425730]

(79). Chang C; Yan J; Yao Z; Zhang C; Li X; Mao HQ Effects of Mesenchymal Stem Cell-Derived Paracrine Signals and Their Delivery Strategies. Adv. Healthcare Mater 2021, 10 (7), 2001689.

(80). Serra-Aguado CI; Llorens-Gamez M; Vercet-Llopis P; Martinez-Chicote V; Deb S; Serrano-Aroca A Engineering Three-Dimensional-Printed Bioactive Polylactic Acid Alginate Composite Scaffolds with Antibacterial and In Vivo Osteoinductive Capacity. ACS Appl. Mater. Interfaces 2022, 14 (48), 53593–53602. [PubMed: 36413629]

(81). Yin J; Zhong J; Wang J; Wang Y; Li T; Wang L; Yang Y; Zhen Z; Li Y; Zhang H; Zhong S; Wu Y; Huang W 3D-printed high-density polyethylene scaffolds with bioactive and antibacterial layer-by-layer modification for auricle reconstruction. Mater. Today Bio 2022, 16, 100361.

(82). Ahmed KS; Ibad H; Suchal ZA; Gosain AK Implementation of 3D Printing and Computer-Aided Design and Manufacturing (CAD/CAM) in Craniofacial Reconstruction. J. Craniofac Surg 2022, 33 (6), 1714–1719. [PubMed: 35165240]

(83). Park SH; Yun BG; Won JY; Yun WS; Shim JH; Lim MH; Kim DH; Baek SA; Alahmari YD; Jeun JH; Hwang SH; Kim SW New application of three-dimensional printing biomaterial in nasal reconstruction. Laryngoscope 2017, 127 (5), 1036–1043. [PubMed: 28150412]

(84). Francisco I; Basilio A; Ribeiro MP; Nunes C; Travassos R; Marques F; Pereira F; Paula AB; Carrilho E; Marto CM; Vale F Three-Dimensional Impression of Biomaterials for Alveolar Graft: Scoping Review. J. Funct Biomater 2023, 14 (2), 76. [PubMed: 36826875]

(85). Goh BT; Teh LY; Tan DB; Zhang Z; Teoh SH Novel 3D polycaprolactone scaffold for ridge preservation–a pilot rando-mised controlled clinical trial. Clin Oral Implants Res. 2015, 26 (3), 271–7. [PubMed: 25263527]

(86). Farris AL; Lambrechts D; Zhou Y; Zhang NY; Sarkar N; Moorer MC; Rindone AN; Nyberg EL; Perdomo-Pantoja A; Burris SJ; Free K; Witham TF; Riddle RC; Grayson WL 3D-printed oxygen-releasing scaffolds improve bone regeneration in mice. Biomaterials 2022, 280, 121318. [PubMed: 34922272]

(87). Hung BP; Naved BA; Nyberg EL; Dias M; Holmes CA; Elisseeff JH; Dorafshar AH; Grayson WL Three-Dimensional Printing of Bone Extracellular Matrix for Craniofacial Regeneration. ACS Biomater Sci. Eng 2016, 2 (10), 1806–1816. [PubMed: 27942578]

(88). Vishwakarma A; Sharpe P; Shi S; Ramalingam M Stem Cell Biology and Tissue Engineering in Dental Sciences, 1st ed.; Academic Press, 2015.

(89). Tetsuka H; Shin SR Materials and technical innovations in 3D printing in biomedical applications. J. Mater. Chem. B 2020, 8 (15), 2930–2950. [PubMed: 32239017]

(90). Pangesty AI; Todo M Improvement of Mechanical Strength of Tissue Engineering Scaffold Due to the Temperature Control of Polymer Blend Solution. J. Funct Biomater 2021, 12 (3), 47. [PubMed: 34449641]

(91). Singh S; Nyberg EL; O'Sullivan AN; Farris A; Rindone AN; Zhang N; Whitehead EC; Zhou Y; Mihaly E; Achebe CC; Zbijewski W; Grundy W; Garlick D; Jackson ND; Taguchi T; Takawira C; Lopez J; Lopez MJ; Grant MP; Grayson WL Point-of-care treatment of geometrically complex midfacial criticalsized bone defects with 3D-Printed scaffolds and autologous stromal vascular fraction. Biomaterials 2022, 282, 121392. [PubMed: 35134701]

(92). Rocha CV; Goncalves V; da Silva MC; Banobre-Lopez M; Gallo J PLGA-Based Composites for Various Biomedical Applications. Int. J. Mol. Sci 2022, 23 (4), 2034. [PubMed: 35216149]

(93). Bergsma EJ; Rozema FR; Bos RR; de Bruijn WC Foreign body reactions to resorbable poly(L-lactide) bone plates and screws used for the fixation of unstable zygomatic fractures. J. Oral Maxillofac Surg 1993, 51 (6), 666–70. [PubMed: 8492205]

(94). Jansen EJ; Sladek RE; Bahar H; Yaffe A; Gijbels MJ; Kuijer R; Bulstra SK; Guldemond NA; Binderman I; Koole LH Hydrophobicity as a design criterion for polymer scaffolds in bone tissue engineering. Biomaterials 2005, 26 (21), 4423–31. [PubMed: 15701371]

(95). da Silva D; Kaduri M; Poley M; Adir O; Krinsky N; Shainsky-Roitman J; Schroeder A Biocompatibility, biodegradation and excretion of polylactic acid (PLA) in medical implants and theranostic systems. Chem. Eng. J 2018, 340, 9–14. [PubMed: 31384170]

(96). Stefaniak K; Masek A Green Copolymers Based on Poly(Lactic Acid)-Short Review. Materials (Basel) 2021, 14 (18), 5254. [PubMed: 34576477]

(97). Generali M; Kehl D; Capulli AK; Parker KK; Hoerstrup SP; Weber B Comparative analysis of poly-glycolic acid-based hybrid polymer starter matrices for in vitro tissue engineering. Colloids Surf. B Biointerfaces 2017, 158, 203–212. [PubMed: 28697435]

(98). Xu H; Han D; Dong JS; Shen GX; Chai G; Yu ZY; Lang WJ; Ai ST Rapid prototyped PGA/PLA scaffolds in the reconstruction of mandibular condyle bone defects. Int. J. Med. Robot 2010, 6 (1), 66–72. [PubMed: 20013824]

(99). Sahar DE; Walker JA; Wang HT; Stephenson SM; Shah AR; Krishnegowda NK; Wenke JC Effect of endothelial differentiated adipose-derived stem cells on vascularity and osteogenesis in poly(D,L-lactide) scaffolds in vivo. J. Craniofac Surg 2012, 23 (3), 913–8. [PubMed: 22627404]

(100). Witek L; Tian H; Tovar N; Torroni A; Neiva R; Gil LF; Coelho PG The effect of platelet-rich fibrin exudate addition to porous poly(lactic-co-glycolic acid) scaffold in bone healing: An in vivo study. J. Biomed Mater. Res. B Appl. Biomater 2020, 108 (4), 1304–1310. [PubMed: 31429195]

(101). Tilton M; Jacobs E; Overdorff R; Astudillo Potes M; Lu L; Manogharan G Biomechanical behavior of PMMA 3D printed biomimetic scaffolds: Effects of physiologically relevant environment. J. Mech Behav Biomed Mater 2023, 138, 105612. [PubMed: 36509012]

(102). Las DE; Verwilghen D; Mommaerts MY A systematic review of cranioplasty material toxicity in human subjects. J. Craniomaxillofac Surg 2021, 49 (1), 34–46. [PubMed: 33257187]

(103). Lee SC; Wu CT; Lee ST; Chen PJ Cranioplasty using polymethyl methacrylate prostheses. J. Clin Neurosci 2009, 16 (1), 56–63. [PubMed: 19046734]

(104). Shah AM; Jung H; Skirboll S Materials used in cranioplasty: a history and analysis. Neurosurg Focus 2014, 36 (4), No. E19. [PubMed: 24684331]

(105). van de Vijfeijken S; Munker T; Spijker R; Karssemakers LHE; Vandertop WP; Becking AG; Ubbink DT; CranioSafe G Autologous Bone Is Inferior to Alloplastic Cranioplasties: Safety of Autograft and Allograft Materials for Cranioplasties, a Systematic Review. World Neurosurg 2018, 117, 443–452. [PubMed: 29879511]

(106). Medical Device Material Performance Study: Polymethyl methacrylate Safety Profile; ECRI, 2021; pp 1–60.

(107). Jain R; Mahendru S; Aggarwal A; Brajesh V; Aulakh HS; Singh S; Jain A; Khazanchi RK Feasibility of Customised Polymethyl Methacrylate Implants Fabricated Using 3D Printed Flexible Moulds for Correction of Facial Skeletal Deformities. J. Craniofac Surg 2021, 32 (6), 1981–1985. [PubMed: 33645954]

(108). Overview of materials for High Density Polyethylene (HDPE), Injection Molded; MatWeb, 2023.

(109). MEDPOR® Oral maxillofacial surgery; Stryker, 2019; pp 1–12.

(110). Nayyer L; Birchall M; Seifalian AM; Jell G Design and development of nanocomposite scaffolds for auricular reconstruction. Nanomedicine 2014, 10 (1), 235–46. [PubMed: 23792331]

(111). Spater T; Menger MD; Laschke MW Vascularization Strategies for Porous Polyethylene Implants. Tissue Eng. Part B Rev 2021, 27 (1), 29–38. [PubMed: 32524897]

(112). Honigmann P; Sharma N; Okolo B; Popp U; Msallem B; Thieringer FM Patient-Specific Surgical Implants Made of 3D Printed PEEK: Material, Technology, and Scope of Surgical Application. Biomed Res. Int 2018, 2018, 4520636. [PubMed: 29713642]

(113). Medical Device Material Performance Study: PEEK Safety Profile; ECRI, 2020; pp 1–92.

(114). Jarvinen S; Suojanen J; Kormi E; Wilkman T; Kiukkonen A; Leikola J; Stoor P The use of patient specific polyetheretherke-tone implants for reconstruction of maxillofacial deformities. J. Craniomaxillofac Surg 2019, 47 (7), 1072–1076. [PubMed: 31103433]

(115). Ma R; Guo D Evaluating the bioactivity of a hydroxyapatite-incorporated polyetheretherketone biocomposite. J. Orthop Surg Res 2019, 14 (1), 32. [PubMed: 30683125]

(116). Thrivikraman G; Athirasala A; Twohig C; Boda SK; Bertassoni LE Biomaterials for Craniofacial Bone Regeneration. Dent Clin North Am. 2017, 61 (4), 835–856. [PubMed: 28886771]

(117). Khalaf AT; Wei Y; Wan J; Zhu J; Peng Y; Abdul Kadir SY; Zainol J; Oglah Z; Cheng L; Shi Z Bone Tissue Engineering through 3D Bioprinting of Bioceramic Scaffolds: A Review and Update. Life (Basel) 2022, 12 (6), 903. [PubMed: 35743934]

(118). Yan Y; Chen H; Zhang H; Guo C; Yang K; Chen K; Cheng R; Qian N; Sandler N; Zhang YS; Shen H; Qi J; Cui W; Deng L Vascularized 3D printed scaffolds for promoting bone regeneration. Biomaterials 2019, 190–191, 97–110.

(119). Ginebra MP; Espanol M; Maazouz Y; Bergez V; Pastorino D Bioceramics and bone healing. EFORT Open Rev. 2018, 3 (5), 173–183. [PubMed: 29951254]

(120). Lopez CD; Diaz-Siso JR; Witek L; Bekisz JM; Cronstein BN; Torroni A; Flores RL; Rodriguez ED; Coelho PG Three dimensionally printed bioactive ceramic scaffold osseoconduction across critical-sized mandibular defects. J. Surg Res 2018, 223, 115–122. [PubMed: 29433862]

(121). Nayak VV; Slavin BV; Bergamo ETP; Torroni A; Runyan CM; Flores RL; Kasper FK; Young S; Coelho PG; Witek L Three-Dimensional Printing Bioceramic Scaffolds Using Direct-Ink-Writing for Craniomaxillofacial Bone Regeneration. Tissue Eng. Part C Methods 2023, 29 (7), 332–345. [PubMed: 37463403]

(122). Lopez CD; Diaz-Siso JR; Witek L; Bekisz JM; Gil LF; Cronstein BN; Flores RL; Torroni A; Rodriguez ED; Coelho PG Dipyridamole Augments Three-Dimensionally Printed Bioactive Ceramic Scaffolds to Regenerate Craniofacial Bone. Plastic and reconstructive surgery 2019, 143 (5), 1408–1419. [PubMed: 31033822]

(123). Lopez CD; Witek L; Torroni A; Flores RL; Demissie DB; Young S; Cronstein BN; Coelho PG The role of 3D printing in treating craniomaxillofacial congenital anomalies. Birth Defects Res. 2018, 110, 1055. [PubMed: 29781248]

(124). Witek L; Alifarag AM; Tovar N; Lopez CD; Cronstein BN; Rodriguez ED; Coelho PG Repair of critical-sized long bone defects using dipyridamole-augmented 3D-printed bioactive ceramic scaffolds. Journal of Orthopaedic Research 2019, 37 (12), 2499–2507. [PubMed: 31334868]

(125). Bekisz JM; Flores RL; Witek L; Lopez CD; Runyan CM; Torroni A; Cronstein BN; Coelho PG Dipyridamole enhances osteogenesis of three-dimensionally printed bioactive ceramic scaffolds in calvarial defects. Journal of cranio-maxillo-facial surgery: official publication of the European Association for Cranio-Maxillo-Facial Surgery 2018, 46, 237. [PubMed: 29292126]

(126). Maliha SG; Lopez CD; Coelho PG; Witek L; Cox M; Meskin A; Rusi S; Torroni A; Cronstein BN; Flores RL Bone Tissue Engineering in the Growing Calvarium Using Dipyridamole-Coated 3D Printed Bioceramic Scaffolds: Construct Optimization and Effects to Cranial Suture Patency. Plast Reconstr Surg 2020, 145, 337e.

(127). Wang MM; Flores RL; Witek L; Torroni A; Ibrahim A; Wang Z; Liss HA; Cronstein BN; Lopez CD; Maliha SG; Coelho PG Dipyridamole-loaded 3D-printed bioceramic scaffolds stimulate pediatric bone regeneration in vivo without disruption of craniofacial growth through facial maturity. Sci. Rep 2019, 9 (1), 18439. [PubMed: 31804544]

(128). Lopez CD; Coelho PG; Witek L; Torroni A; Greenberg MI; Cuadrado DL; Guarino AM; Bekisz JM; Cronstein BN; Flores RL Regeneration of a pediatric alveolar cleft model using three-dimensionally printed bioceramic scaffolds and osteogenic agents: comparison of dipyridamole and rhBMP-2. Plastic and reconstructive surgery 2019, 144 (2), 358–370. [PubMed: 31348344]

(129). Fama C; Kaye GJ; Flores R; Lopez CD; Bekisz JM; Torroni A; Tovar N; Coelho PG; Witek L Three-Dimensionally-Printed Bioactive Ceramic Scaffolds: Construct Effects on Bone Regeneration. Journal of Craniofacial Surgery 2021, 32 (3), 1177–1181. [PubMed: 33003153]

(130). Shen C; Wang MM; Witek L; Tovar N; Cronstein BN; Torroni A; Flores RL; Coelho PG Transforming the degradation rate of β-tricalcium phosphate bone replacement using 3-dimensional printing. Annals of Plastic Surgery 2021, 87 (6), No. e153–e162. [PubMed: 34611100]

(131). Shen C; Wang MM; Witek L; Tovar N; Cronstein BN; Torroni A; Flores RL; Coelho PG Transforming the Degradation Rate of beta-tricalcium Phosphate Bone Replacement Using 3-Dimensional Printing. Ann. Plast Surg 2021, 87 (6), No. e153–e162. [PubMed: 34611100]

(132). James AW; LaChaud G; Shen J; Asatrian G; Nguyen V; Zhang X; Ting K; Soo C A Review of the Clinical Side Effects of Bone Morphogenetic Protein-2. Tissue Eng. Part B Rev 2016, 22 (4), 284–97. [PubMed: 26857241]

(133). Grant GT; Rybicki FJ 3D Printing in Medicine: A Practical Guide for Medical Professionals, 1st ed.; Springer International Publishing: Cham, 2017.

(134). Pagac M; Hajnys J; Ma QP; Jancar L; Jansa J; Stefek P; Mesicek J A Review of Vat Photopolymerization Technology: Materials, Applications, Challenges, and Future Trends of 3D Printing. Polymers (Basel) 2021, 13 (4), 598. [PubMed: 33671195]

(135). Al Rashid A; Ahmed W; Khalid MY; Koç M Vat photopolymerization of polymers and polymer composites: Processes and applications. Additive Manufacturing 2021, 47, 102279.

(136). Hann SY; Cui H; Esworthy T; Zhou X; Lee SJ; Plesniak MW; Zhang LG Dual 3D printing for vascularized bone tissue regeneration. Acta Biomater 2021, 123, 263–274. [PubMed: 33454383]

(137). Le Guehennec L; Van Hede D; Plougonven E; Nolens G; Verlee B; De Pauw MC; Lambert F In vitro and in vivo biocompatibility of calcium-phosphate scaffolds three-dimensional printed by stereolithography for bone regeneration. J. Biomed Mater. Res. A 2020, 108 (3), 412–425. [PubMed: 31654476]

(138). Obregon F; Vaquette C; Ivanovski S; Hutmacher DW; Bertassoni LE Three-Dimensional Bioprinting for Regenerative Dentistry and Craniofacial Tissue Engineering. Journal of Dental Research 2015, 94 (9_suppl), 143S–152S. [PubMed: 26124216]

(139). Gulcan O; Gunaydin K; Tamer A The State of the Art of Material Jetting-A Critical Review. Polymers (Basel) 2021, 13 (16), 2829. [PubMed: 34451366]

(140). Meglioli M; Naveau A; Macaluso GM; Catros S 3D printed bone models in oral and cranio-maxillofacial surgery: a systematic review. 3D Print Med. 2020, 6 (1), 30. [PubMed: 33079298]

(141). Chondro-Gide; Geistlich, 2023. https://www.geistlich-pharma.com/orthopedic/cartilage-regeneration/general-information/chondro-gide#:~:text=Chondro%2DGide%C2%AE%20works%20to,the%20conditions%20for%20cartilage%20regeneration (accessed July 10, 2023).

(142). Chen L; Lin WS; Polido WD; Eckert GJ; Morton D Accuracy, reproducibility, and dimensional stability of additively manufactured surgical templates. J. Prosthet Dent 2019, 122 (3), 309–314. [PubMed: 30948293]

(143). Kim T; Lee S; Kim GB; Hong D; Kwon J; Park JW; Kim N Accuracy of a simplified 3D-printed implant surgical guide. J. Prosthet Dent 2020, 124 (2), 195–201. [PubMed: 31753464]

(144). Chen YW; Fang HY; Shie MY; Shen YF The mussel-inspired assisted apatite mineralized on PolyJet material for artificial bone scaffold. Int. J. Bioprint 2019, 5 (2), 197. [PubMed: 32596535]

(145). Miljanovic D; Seyedmahmoudian M; Stojcevski A; Horan B Design and Fabrication of Implants for Mandibular and Craniofacial Defects Using Different Medical-Additive Manufacturing Technologies: A Review. Ann. Biomed Eng 2020, 48 (9), 2285–2300. [PubMed: 32691264]

(146). Zhang J; Vasiliauskaite E; De Kuyper A; De Schryver C; Vogeler F; Desplentere F; Ferraris E Temperature Analyses in Fused Filament Fabrication: From Filament Entering the Hot-End to the Printed Parts. 3D Print Addit Manuf 2022, 9 (2), 132–142. [PubMed: 36655000]

(147). Turek P; Budzik G Estimating the Accuracy of Mandible Anatomical Models Manufactured Using Material Extrusion Methods. Polymers (Basel) 2021, 13 (14), 2271. [PubMed: 34301029]

(148). Winarso R; Anggoro PW; Ismail R; Jamari J; Bayuseno AP Application of fused deposition modeling (FDM) on bone scaffold manufacturing process: A review. Heliyon 2022, 8 (11), No. e11701. [PubMed: 36444266]

(149). Cheng D; Yuan M; Perera I; O'Connor A; Evins AI; Imahiyerobo T; Souweidane M; Hoffman C Developing a 3D composite training model for cranial remodeling. J. Neurosurg Pediatr 2019, 24, 1–10. [PubMed: 30952115]

(150). Flores RL; Liss H; Raffaelli S; Humayun A; Khouri KS; Coelho PG; Witek L The technique for 3D printing patient-specific models for auricular reconstruction. J. Craniomaxillofac Surg 2017, 45 (6), 937–943. [PubMed: 28465028]

(151). Ciocca L; Fantini M; De Crescenzio F; Persiani F; Scotti R Computer-aided design and manufacturing construction of a surgical template for craniofacial implant positioning to support a definitive nasal prosthesis. Clin Oral Implants Res. 2011, 22 (8), 850–6. [PubMed: 21198902]

(152). Petropolis C; Kozan D; Sigurdson L Accuracy of medical models made by consumer-grade fused deposition modelling printers. Plast Surg (Oakv) 2015, 23 (2), 91–4. [PubMed: 26090349]

(153). Saadi M; Maguire A; Pottackal NT; Thakur MSH; Ikram MM; Hart AJ; Ajayan PM; Rahman MM Direct Ink Writing: A 3D Printing Technology for Diverse Materials. Adv. Mater 2022, 34 (28), No. e2108855. [PubMed: 35246886]

(154). Elsayed H; Rebesan P; Giacomello G; Pasetto M; Gardin C; Ferroni L; Zavan B; Biasetto L Direct ink writing of porous titanium (Ti6Al4V) lattice structures. Mater. Sci. Eng. C Mater. Biol. Appl 2019, 103, 109794. [PubMed: 31349412]

(155). Wang Y; Muller WD; Rumjahn A; Schwitalla A Parameters Influencing the Outcome of Additive Manufacturing of Tiny Medical Devices Based on PEEK. Materials (Basel) 2020, 13 (2), 466. [PubMed: 31963725]

(156). Awad A; Fina F; Goyanes A; Gaisford S; Basit AW Advances in powder bed fusion 3D printing in drug delivery and healthcare. Adv. Drug Deliv Rev 2021, 174, 406–424. [PubMed: 33951489]

(157). Yanez A; Fiorucci MP; Martel O; Cuadrado A The Influence of Dimensions and Powder Recycling on the Roughness and Mechanical Properties of Ti-6Al-4V Parts Fabricated by Laser Powder Bed Fusion. Materials (Basel) 2022, 15 (16), 5787. [PubMed: 36013922]

(158). Liao HT; Lee MY; Tsai WW; Wang HC; Lu WC Osteogenesis of adipose-derived stem cells on polycaprolactone-beta-tricalcium phosphate scaffold fabricated via selective laser sintering and surface coating with collagen type I. J. Tissue Eng. Regen Med 2016, 10 (10), No. E337–E353. [PubMed: 23955935]

(159). Bernhardt A; Schneider J; Schroeder A; Papadopoulous K; Lopez E; Bruckner F; Botzenhart U Surface conditioning of additively manufactured titanium implants and its influence on materials properties and in vitro biocompatibility. Mater. Sci. Eng. C Mater. Biol. Appl 2021, 119, 111631. [PubMed: 33321670]

(160). Nemtoi A; Covrig V; Nemtoi A; Stoica G; Vatavu R; Haba D; Zetu I Custom-Made Direct Metal Laser Sintering Titanium Subperiosteal Implants in Oral and Maxillofacial Surgery for Severe Bone-Deficient Patients-A Pilot Study. Diagnostics (Basel) 2022, 12 (10), 2531. [PubMed: 36292220]

(161). Suojanen J; Jarvinen S; Kotaniemi KV; Reunanen J; Palotie T; Stoor P; Leikola J Comparison between patient specific implants and conventional mini-plates in Le Fort I osteotomy with regard to infections: No differences in up to 3-year follow-up. J. Craniomaxillofac Surg 2018, 46 (10), 1814–1817. [PubMed: 30097411]

(162). Shilo D; Capucha T; Blanc O; Shilo Yaacobi D; Emodi O; Rachmiel A Patient-specific Implants for Treating Atrophic Mandibles. Plast Reconstr Surg Glob Open 2022, 10 (6), No. e4359. [PubMed: 35685746]

(163). Morrison RJ; Kashlan KN; Flanangan CL; Wright JK; Green GE; Hollister SJ; Weatherwax KJ Regulatory Considerations in the Design and Manufacturing of Implantable 3D-Printed Medical Devices. Clin Transl Sci. 2015, 8 (5), 594–600. [PubMed: 26243449]

(164). Sastri VR Plastics in medical devices: properties, requirements, and applications; Elsevier, 2014.

(165). U.S. FDA Submission and Review of Sterility Information in Premarket Notification (510(k)) Submissions for Devices Labeled as Sterile; Center for Devices and Radiological Health, 2016; pp 1–11.

(166). Klammert U; Gbureck U; Vorndran E; Rodiger J; Meyer-Marcotty P; Kubler AC 3D powder printed calcium phosphate implants for reconstruction of cranial and maxillofacial defects. J. Craniomaxillofac Surg 2010, 38 (8), 565–70. [PubMed: 20206538]

(167). Sharma N; Zubizarreta-Oteiza J; Tourbier C; Thieringer FM Can Steam Sterilization Affect the Accuracy of Point-of-Care 3D Printed Polyetheretherketone (PEEK) Customized Cranial Implants? An Investigative Analysis. J. Clin Med 2023, 12 (7), 2495. [PubMed: 37048579]

(168). Munker T; van de Vijfeijken S; Mulder CS; Vespasiano V; Becking AG; Kleverlaan CJ; CranioSafe G; CranioSafe G; Becking AG; Dubois L; Karssemakers LHE; Milstein DMJ; van de Vijfeijken S; Depauw P; Hoefnagels FWA; Vandertop WP; Kleverlaan CJ; Munker T; Maal TJJ; Nout E; Riool M; Zaat SAJ Effects of sterilization on the mechanical properties of poly(methyl methacrylate) based personalized medical devices. J. Mech Behav Biomed Mater 2018, 81, 168–172. [PubMed: 29524755]

(169). Told R; Ujfalusi Z; Pentek A; Kerenyi M; Banfai K; Vizi A; Szabo P; Melegh S; Bovari-Biri J; Pongracz JE; Maroti P A state-of-the-art guide to the sterilization of thermoplastic polymers and resin materials used in the additive manufacturing of medical devices. Materials & design 2022, 223, 111119.

(170). Chernonosova VS; Kuzmin IE; Shundrina IK; Korobeynikov MV; Golyshev VM; Chelobanov BP; Laktionov PP Effect of Sterilization Methods on Electrospun Scaffolds Produced from Blend of Polyurethane with Gelatin. J. Funct Biomater 2023, 14 (2), 70. [PubMed: 36826869]

(171). Bruyas A; Moeinzadeh S; Kim S; Lowenberg DW; Yang YP Effect of Electron Beam Sterilization on Three-Dimensional-Printed Polycaprolactone/Beta-Tricalcium Phosphate Scaffolds for Bone Tissue Engineering. Tissue Eng. Part A 2019, 25 (3–4), 248–256. [PubMed: 30234441]

(172). Li X; Guo B; Xiao Y; Yuan T; Fan Y; Zhang X Influences of the steam sterilization on the properties of calcium phosphate porous bioceramics. J. Mater. Sci. Mater. Med 2016, 27 (1), 5. [PubMed: 26610928]

(173). Ballard DH; Mills P; Duszak R Jr; Weisman JA; Rybicki FJ; Woodard PK Medical 3D Printing Cost-Savings in Orthopedic and Maxillofacial Surgery: Cost Analysis of Operating Room Time Saved with 3D Printed Anatomic Models and Surgical Guides. Acad. Radiol 2020, 27 (8), 1103–1113. [PubMed: 31542197]

(174). 3D Printing Medical Devices Market; MarketsandMarkets, 2023; pp 1–346.

(175). Michas F Hospitals with 3D printing facilities in the US 2010 – 2019; Materialise: Statista, 2021.

(176). Aniwaa 3D printer catalog; Aniwaa, 2023. https://www.aniwaa.com/catalog/3d-printers/? (accessed 07-19-2023).

(177). Formlabs Guide to 3D Printing Medical Devices: From Prototyping to Commercialization; Formlabs, 2023. https://formlabs.com/blog/3d-printing-medical-devices/ (accessed 07-19-2023).

(178). Lau I; Wong YH; Yeong CH; Abdul Aziz YF; Md Sari NA; Hashim SA; Sun Z Quantitative and qualitative comparison of low- and high-cost 3D-printed heart models. Quant Imaging Med. Surg 2019, 9 (1), 107–114. [PubMed: 30788252]

(179). Hatz CR; Msallem B; Aghlmandi S; Brantner P; Thieringer FM Can an entry-level 3D printer create high-quality anatomical models? Accuracy assessment of mandibular models printed by a desktop 3D printer and a professional device. Int. J. Oral Maxillofac Surg 2020, 49 (1), 143–148. [PubMed: 31300302]

(180). Polylactic acid (PLA) price index; Business Analyt IQ, 2023. https://businessanalytiq.com/procurementanalytics/index/polylactic-acid-pla-price-index/ (accessed 07-19-2023).

(181). PEEK Filament; 3D4Makers, 2023. https://www.3d4makers.com/products/peek-filament (accessed 07-19-2023).

(182). HDPE price index; Business Analyt IQ, 2023. https://businessanalytiq.com/procurementanalytics/index/hdpe-price-index/ (accessed 07-19-2023).

(183). Polymethylmethacrylate (PMMA) price index; Business Analyt IQ, 2023. https://businessanalytiq.com/procurementanalytics/index/polymethylmethacrylate-pmma-price-index/ (accessed 07-19-2023).

(184). Titanium; Trading Economics, 2023. https://tradingeconomics.com/commodity/titanium (accessed 07-19-2023).

(185). Ravi P; Burch MB; Farahani S; Chepelev LL; Yang D; Ali A; Joyce JR; Lawera N; Stringer J; Morris JM; Ballard DH; Wang KC; Mahoney MC; Kondor S; Rybicki FJ; et al. University of Cincinnati, D. P. C. S. P., Utility and Costs During the Initial Year of 3D Printing in an Academic Hospital. J. Am. Coll Radiol 2023, 20 (2), 193–204. [PubMed: 35988585]

(186). Wilde F; Hanken H; Probst F; Schramm A; Heiland M; Cornelius CP Multicenter study on the use of patient-specific CAD/CAM reconstruction plates for mandibular reconstruction. Int. J. Comput. Assist Radiol Surg 2015, 10 (12), 2035–51. [PubMed: 25843949]

(187). Bell RB; Weimer KA; Dierks EJ; Buehler M; Lubek JE Computer planning and intraoperative navigation for palatomaxillary and mandibular reconstruction with fibular free flaps. J. Oral Maxillofac Surg 2011, 69 (3), 724–32. [PubMed: 20888108]

(188). Antony AK; Chen WF; Kolokythas A; Weimer KA; Cohen MN Use of virtual surgery and stereolithography-guided osteotomy for mandibular reconstruction with the free fibula. Plast Reconstr Surg 2011, 128 (5), 1080–1084. [PubMed: 22030490]

(189). Dumas BM; Nava A; Law HZ; Smartt J; Derderian C; Seaward JR; Kane AA; Hallac RR Three-Dimensional Printing for Craniofacial Surgery: A Single Institution's 5-Year Experience. Cleft Palate Craniofac J. 2019, 56 (6), 729–734. [PubMed: 30200785]

(190). Mendez BM; Chiodo MV; Patel PA Customized ″In-Office″ Three-Dimensional Printing for Virtual Surgical Planning in Craniofacial Surgery. J. Craniofac Surg 2015, 26 (5), 1584–6. [PubMed: 26106998]

(191). Marques MA; Purnell CA; Zhao L; Patel PK; Alkureishi LWT Patient-specific Composite Anatomic Models: Improving the Foundation for Craniosynostosis Repair. J. Craniofac Surg 2023, 34 (3), 1078–1081. [PubMed: 36727996]

(192). Barreda Hale M; Romero-Araya P; Cea Herrera M; Espinoza D; Castro N; Castro J; Serandour G Computer-assisted planning with 3D printing for mandibular reconstruction caused by a mandibular fracture with secondary osteomyelitis: A Case Report. Clin Case Rep 2021, 9 (7), No. e04410. [PubMed: 34295476]

(193). Bekisz JM; Liss HA; Maliha SG; Witek L; Coelho PG; Flores RL In-House Manufacture of Sterilizable, Scaled, Patient-Specific 3D-Printed Models for Rhinoplasty. Aesthet Surg J. 2019, 39 (3), 254–263. [PubMed: 29982464]

(194). Telich-Tarriba JE; Chavez-Serna E; Rangel-Rangel E; Gorostieta-Esperon MA; Andrade Delgado L; Fuente Del Campo A Surgical Planning for Mandibular Distraction Osteogenesis Using Low-Cost Three-Dimensional-Printed Anatomic Models. J. Craniofac Surg 2020, 31 (4), No. e319–e321. [PubMed: 32028363]

(195). Sharaf B; Morris J; Vyas KS Point of Care Virtual Surgical Planning and Three-Dimensional Printing for Feminizing Forehead-plasty. Plast Reconstr Surg 2021, 148 (6), 1080e–1082e.

(196). Arias E; Huang YH; Zhao L; Seelaus R; Patel P; Cohen M Virtual Surgical Planning and Three-Dimensional Printed Guide for Soft Tissue Correction in Facial Asymmetry. J. Craniofac Surg 2019, 30 (3), 846–850. [PubMed: 30817522]

(197). Hanasono MM; Skoracki RJ Computer-assisted design and rapid prototype modeling in microvascular mandible reconstruction. Laryngoscope 2013, 123 (3), 597–604. [PubMed: 23007556]

(198). Kim DH; Lee IH; Yun WS; Shim JH; Choi D; Hwang SH; Kim SW Long-term efficacy and safety of 3D printed implant in patients with nasal septal deformities. Eur. Arch Otorhinolaryngol 2022, 279 (4), 1943–1950. [PubMed: 34291346]

(199). Nahumi N; Shohet MR; Bederson JB; Elahi E Frontorbital Fibrous Dysplasia Resection and Reconstruction With Custom Polyetherlatone Alloplast. J. Craniofac Surg 2015, 26 (8), No. e720. [PubMed: 26594985]

(200). Stoor P; Suomalainen A; Lindqvist C; Mesimaki K; Danielsson D; Westermark A; Kontio RK Rapid prototyped patient specific implants for reconstruction of orbital wall defects. J. Craniomaxillofac Surg 2014, 42 (8), 1644–9. [PubMed: 25139812]

(201). Mangano C; Bianchi A; Mangano FG; Dana J; Colombo M; Solop I; Admakin O Custom-made 3D printed subperiosteal titanium implants for the prosthetic restoration of the atrophic posterior mandible of elderly patients: a case series. 3D Print Med. 2020, 6 (1), 1. [PubMed: 31915946]

(202). Suojanen J; Leikola J; Stoor P The use of patient-specific implants in orthognathic surgery: A series of 32 maxillary osteotomy patients. J. Craniomaxillofac Surg 2016, 44 (12), 1913–1916. [PubMed: 27769722]

(203). Yang WF; Choi WS; Wong MC; Powcharoen W; Zhu WY; Tsoi JK; Chow M; Kwok KW; Su YX Three-Dimensionally Printed Patient-Specific Surgical Plates Increase Accuracy of Oncologic Head and Neck Reconstruction Versus Conventional Surgical Plates: A Comparative Study. Ann. Surg Oncol 2021, 28 (1), 363–375. [PubMed: 32572853]

(204). Yoo HJ; Hartsfield JK Jr; Mian AS; Allan BP; Naoum S; Lee RJH; Goonewardene MS Accuracy of mandibular repositioning surgery using new technology: Computer-aided design and manufacturing customized surgical cutting guides and fixation plates. Am. J. Orthod Dentofacial Orthop 2023, 163 (3), 357–367. [PubMed: 36503861]

(205). Fleury CM; Sayyed AA; Baker SB Custom Plates in Orthognathic Surgery: A Single Surgeon's Experience and Learning Curve. J. Craniofac Surg 2022, 33 (7), 1976–1981. [PubMed: 35184108]

(206). Demes E; Rios O; Chamorey E; Lerhe B; D'Andrea G; Savoldelli C Accuracy of mandibular anterior subapical osteotomy by virtual planning in orthognathic surgery using patient-specific implants. J. Stomatol Oral Maxillofac Surg 2023, 124 (1S), 101299. [PubMed: 36184071]

(207). Yang HJ; Oh JH Reconstruction of Mandibular Contour Defect Using Patient-Specific Titanium Implant Manufactured by Selective Laser Melting Method. J. Craniofac Surg 2022, 33 (7), 2055–2058. [PubMed: 36201699]

(208). Olate S; Uribe F; Huentequeo-Molina C; Goulart DR; Sigua-Rodriguez EA; Alister JP Mandibular Angle Contouring Using Porous Polyethylene Stock or PEEK-based Patient Specific Implants. A Critical Analysis. J. Craniofac Surg 2021, 32 (1), 242–246. [PubMed: 32858611]

(209). Park EK; Lim JY; Yun IS; Kim JS; Woo SH; Kim DS; Shim KW Cranioplasty Enhanced by Three-Dimensional Printing: Custom-Made Three-Dimensional-Printed Titanium Im-plants for Skull Defects. J. Craniofac Surg 2016, 27 (4), 943–9. [PubMed: 27192643]

(210). Jonkergouw J; van de Vijfeijken SE; Nout E; Theys T; Van de Casteele E; Folkersma H; Depauw PR; Becking AG Outcome in patient-specific PEEK cranioplasty: A two-center cohort study of 40 implants. J. Craniomaxillofac Surg 2016, 44 (9), 1266–72. [PubMed: 27524384]

(211). Manrique OJ; Lalezarzadeh F; Dayan E; Shin J; Buchbinder D; Smith M Craniofacial reconstruction using patient-specific implants polyether ether ketone with computer-assisted planning. J. Craniofac Surg 2015, 26 (3), 663–6. [PubMed: 25974770]

(212). Rammos CK; Cayci C; Castro-Garcia JA; Feiz-Erfan I; Lettieri SC Patient-specific polyetheretherketone implants for repair of craniofacial defects. J. Craniofac Surg 2015, 26 (3), 631–3. [PubMed: 25901667]

(213). Brie J; Chartier T; Chaput C; Delage C; Pradeau B; Caire F; Boncoeur MP; Moreau JJ A new custom made bioceramic implant for the repair of large and complex craniofacial bone defects. J. Craniomaxillofac Surg 2013, 41 (5), 403–7. [PubMed: 23218977]

(214). Cho KH; Papay FA; Yanof J; West K; Bassiri Gharb B; Rampazzo A; Gastman B; Schwarz GS Mixed Reality and 3D Printed Models for Planning and Execution of Face Transplantation. Ann. Surg 2021, 274 (6), No. e1238–e1246. [PubMed: 32224738]

(215). Chou PY; Hallac RR; Shih E; Trieu J; Penumatcha A; Das P; Meyer CA; Seaward JR; Kane AA 3D-Printed Models of Cleft Lip and Palate for Surgical Training and Patient Education. Cleft Palate Craniofac J. 2018, 55 (3), 323–327. [PubMed: 29437509]

(216). Coelho G; Chaves TMF; Goes AF; Del Massa EC; Moraes O; Yoshida M Multimaterial 3D printing preoperative planning for frontoethmoidal meningoencephalocele surgery. Childs Nerv Syst 2018, 34 (4), 749–756. [PubMed: 29067504]

(217). Engel M; Hoffmann J; Castrillon-Oberndorfer G; Freudlsperger C The value of three-dimensional printing modelling for surgical correction of orbital hypertelorism. Oral Maxillofac Surg 2015, 19 (1), 91–5. [PubMed: 25249178]

(218). Seruya M; Borsuk DE; Khalifian S; Carson BS; Dalesio NM; Dorafshar AH Computer-aided design and manufacturing in craniosynostosis surgery. J. Craniofac Surg 2013, 24 (4), 1100–5. [PubMed: 23851748]

(219). Garcia-Mato D; Ochandiano S; Garcia-Sevilla M; Navarro-Cuellar C; Darriba-Alles JV; Garcia-Leal R; Calvo-Haro JA; Perez-Mananes R; Salmeron JI; Pascau J Craniosynostosis surgery: workflow based on virtual surgical planning, intraoperative navigation and 3D printed patient-specific guides and templates. Sci. Rep 2019, 9 (1), 17691. [PubMed: 31776390]

(220). Manninen AA; Tornwall J; Horelli JC; Heliovaara AK; Mesimaki KV; Lindford AJ; Wilkman TSE; Lassus P Virtual 3D planning and prediction accuracy in two bimaxillary face trans-plantations in Helsinki. J. Plast Reconstr Aesthet Surg 2022, 75 (2), 605–612. [PubMed: 34794919]

(221). Doscher ME; Garfein ES; Bent J; Tepper OM Neonatal mandibular distraction osteogenesis: converting virtual surgical planning into an operative reality. Int. J. Pediatr Otorhinolaryngol 2014, 78 (2), 381–4. [PubMed: 24374142]

(222). Swendseid BP; Roden DF; Vimawala S; Richa T; Sweeny L; Goldman RA; Luginbuhl A; Heffelfinger RN; Khanna S; Curry JM Virtual Surgical Planning in Subscapular System Free Flap Reconstruction of Midface Defects. Oral Oncol 2020, 101, 104508. [PubMed: 31864958]

(223). Kuruoglu D; Yan M; Bustos SS; Morris JM; Alexander AE; Sharaf B Point of care virtual surgical planning and 3D printing in facial gender confirmation surgery: a narrative review. Ann. Transl Med 2021, 9 (7), 614. [PubMed: 33987312]

(224). Li J; Gsaxner C; Pepe A; Morais A; Alves V; von Campe G; Wallner J; Egger J Synthetic skull bone defects for automatic patient-specific craniofacial implant design. Sci. Data 2021, 8 (1), 36. [PubMed: 33514740]

(225). Kaplan N; Marques M; Scharf I; Yang K; Alkureishi L; Purnell C; Patel P; Zhao L Virtual Reality and Augmented Reality in Plastic and Craniomaxillofacial Surgery: A Scoping Review. Bioengineering (Basel) 2023, 10 (4), 480. [PubMed: 37106667]

(226). Coelho G; Rabelo NN; Vieira E; Mendes K; Zagatto G; Santos de Oliveira R; Raposo-Amaral CE; Yoshida M; de Souza MR; Fagundes CF; Teixeira MJ; Figueiredo EG Augmented reality and physical hybrid model simulation for preoperative planning of metopic craniosynostosis surgery. Neurosurg Focus 2020, 48 (3), No. E19.

(227). Waked K; Mespreuve M; De Ranter J; Collard B; Hahn S; Hendrickx B Visualizing the Individual Arterial Anatomy of the Face Through Augmented Reality- A Useful and Accurate Tool During Dermal Filler Injections. Aesthet Surg J. Open Forum 2022, 4, ojac012. [PubMed: 35517577]

(228). Nuri T; Mitsuno D; Otsuki Y; Ueda K Augmented Reality Technology for the Positioning of the Auricle in the Treatment of Microtia. Plast Reconstr Surg Glob Open 2020, 8 (2), No. e2626. [PubMed: 32309078]

(229). Han JJ; Sodnom-Ish B; Eo MY; Kim YJ; Oh JH; Yang HJ; Kim SM Accurate Mandible Reconstruction by Mixed Reality, 3D Printing, and Robotic-Assisted Navigation Integration. J. Craniofac Surg 2022, 33 (6), No. e701–e706. [PubMed: 35240669]

(230). MacAdam A; Chaudry E; McTiernan CD; Cortes D; Suuronen EJ; Alarcon EI Development of in situ bioprinting: A mini review. Front Bioeng Biotechnol 2022, 10, 940896. [PubMed: 35935512]

(231). Kerouredan O; Hakobyan D; Remy M; Ziane S; Dusserre N; Fricain JC; Delmond S; Thebaud NB; Devillard R In situ prevascularization designed by laser-assisted bioprinting: effect on bone regeneration. Biofabrication 2019, 11 (4), 045002. [PubMed: 31151125]

(232). Keriquel V; Guillemot F; Arnault I; Guillotin B; Miraux S; Amedee J; Fricain JC; Catros S In vivo bioprinting for computer- and robotic-assisted medical intervention: preliminary study in mice. Biofabrication 2010, 2 (1), 014101. [PubMed: 20811116]

(233). Keriquel V; Oliveira H; Remy M; Ziane S; Delmond S; Rousseau B; Rey S; Catros S; Amedee J; Guillemot F; Fricain JC In situ printing of mesenchymal stromal cells, by laser-assisted bioprinting, for in vivo bone regeneration applications. Sci. Rep 2017, 7 (1), 1778. [PubMed: 28496103]

(234). Miao S; Castro N; Nowicki M; Xia L; Cui H; Zhou X; Zhu W; Lee SJ; Sarkar K; Vozzi G; Tabata Y; Fisher J; Zhang LG 4D printing of polymeric materials for tissue and organ regeneration. Mater. Today (Kidlington) 2017, 20 (10), 577–591. [PubMed: 29403328]

(235). Senatov FS; Niaza KV; Zadorozhnyy MY; Maksimkin AV; Kaloshkin SD; Estrin YZ Mechanical properties and shape memory effect of 3D-printed PLA-based porous scaffolds. J. Mech Behav Biomed Mater 2016, 57, 139–48. [PubMed: 26710259]

(236). Xie R; Hu J; Hoffmann O; Zhang Y; Ng F; Qin T; Guo X Self-fitting shape memory polymer foam inducing bone regeneration: A rabbit femoral defect study. Biochim Biophys Acta Gen Subj 2018, 1862 (4), 936–945. [PubMed: 29360569]

(237). Morrison RJ; Hollister SJ; Niedner MF; Mahani MG; Park AH; Mehta DK; Ohye RG; Green GE Mitigation of tracheobronchomalacia with 3D-printed personalized medical devices in pediatric patients. Sci. Transl Med 2015, 7 (285), 285ra64.

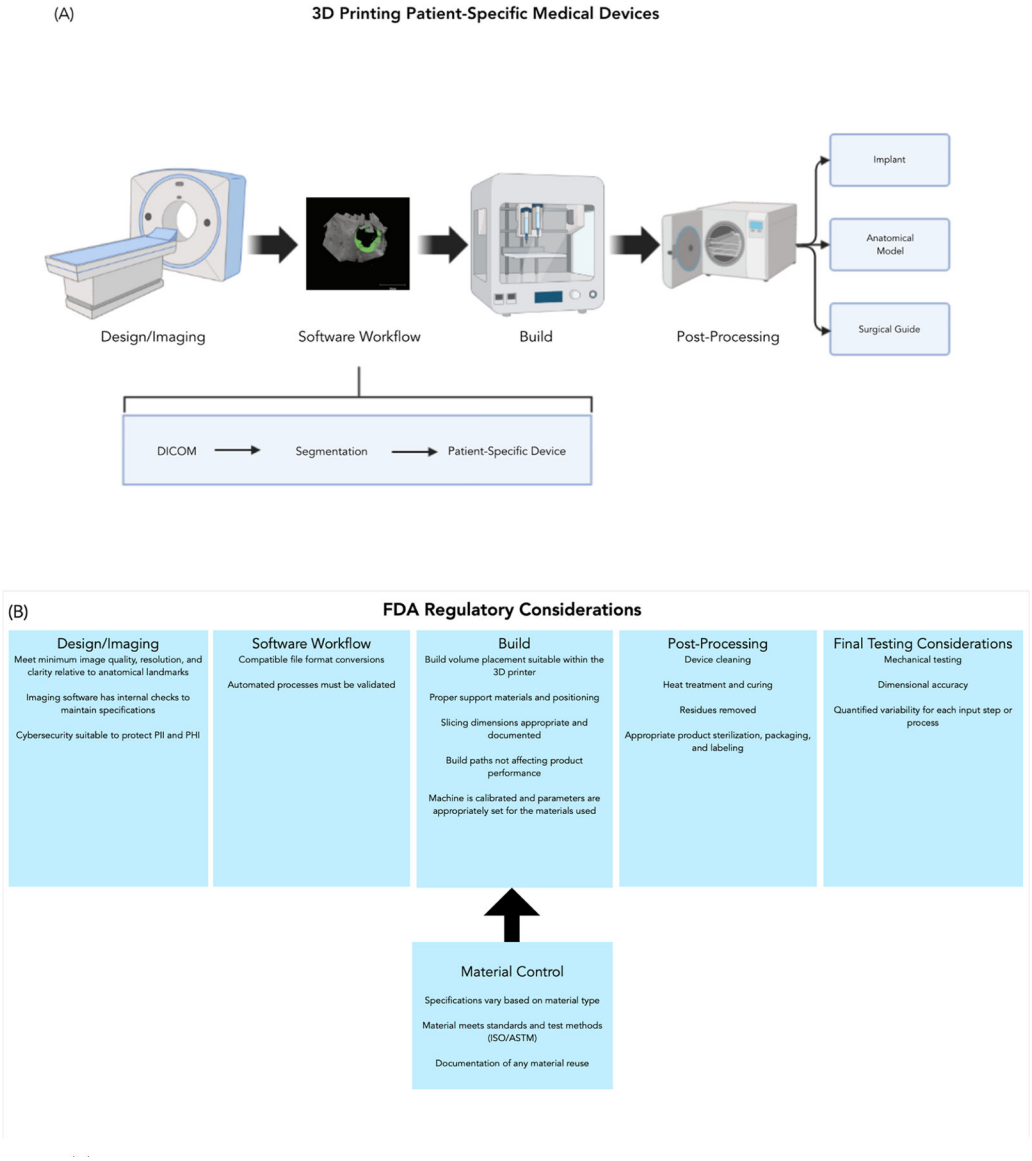

Figure 1.

(A) The 3DP workflow is for manufacturing a patient-specific anatomical model, surgical guide, or implant. CT/MRI data are converted to a DICOM[36] and further processed in preparation for design, printing, and postprocessing. (B) This highlights the critical phases of the 3DMD workflow that are overseen by the FDA. Within each phase, the FDA emphasizes specifications that must be considered for approval of a premarket device. Created with BioRender.com.

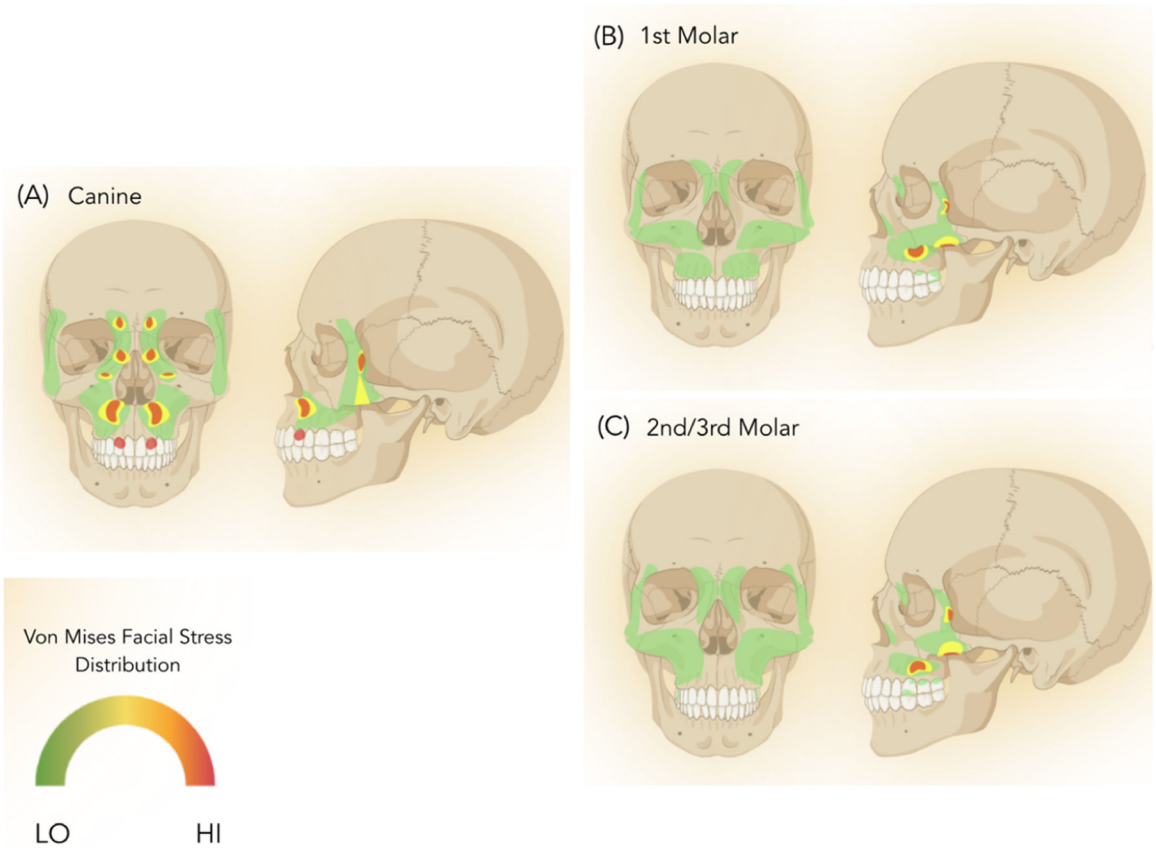

Figure 2.

Representation of Von Mises stress distribution across the facial skeleton based upon bite point at the (A) canine, (B) 1st molar, or (C) 2nd/3rd molars. Green and red depict low and high areas of stress, respectively. Created with BioRender.com.

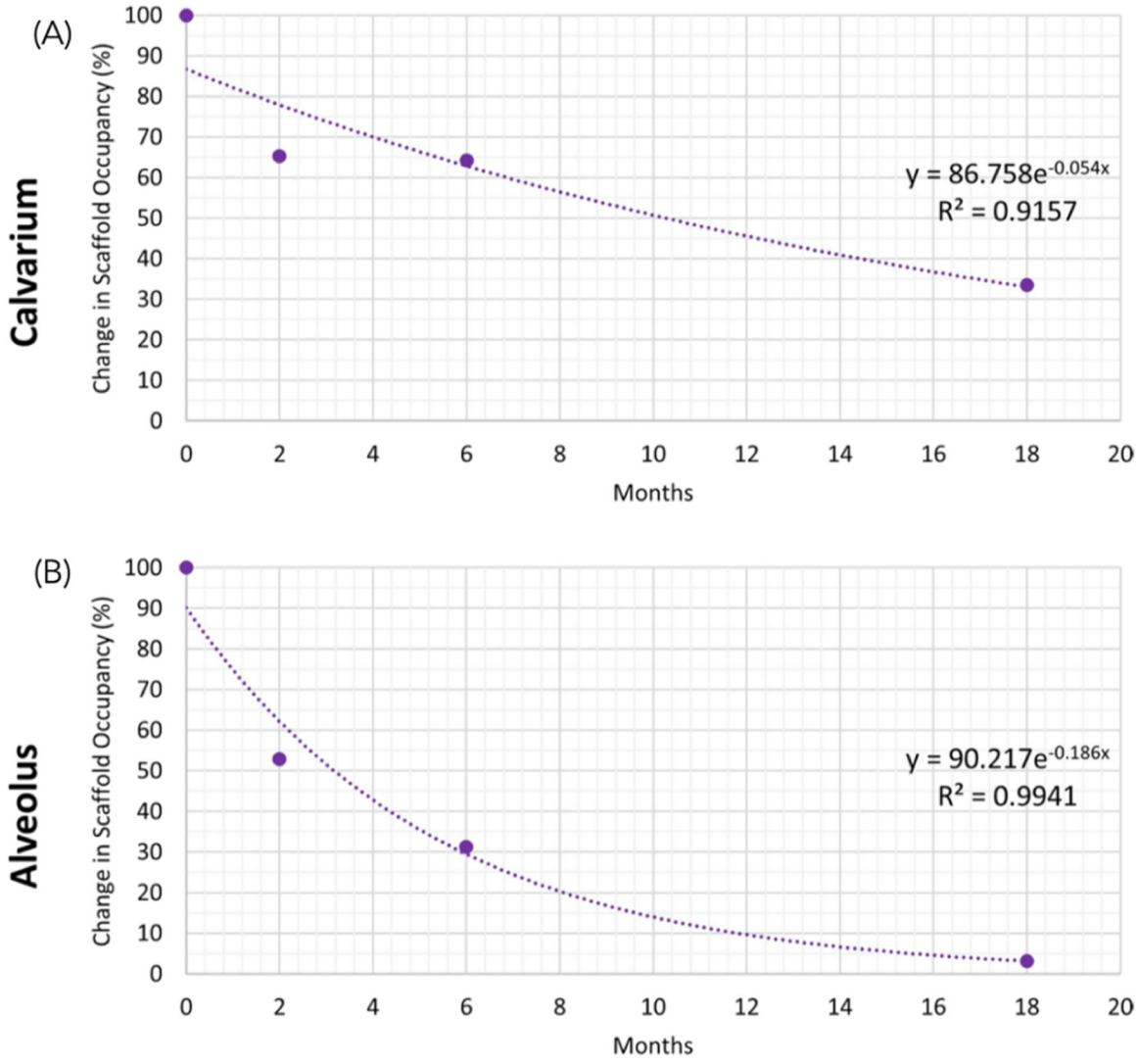

Figure 3.

A drawback of 3D printed bioceramics for targeted bone regeneration is their resorption kinetics. With the addition of a 1000 μM DIPY coating, Shen et al. successfully altered the degradation rate of β-TCP scaffolds to 55%/year and 90%/year within (A) calvarial and (B) alveolar defects, respectively, in a rabbit model. Reproduced from ref 131. Copyright 2023, Wolters Kluwer Health Inc.

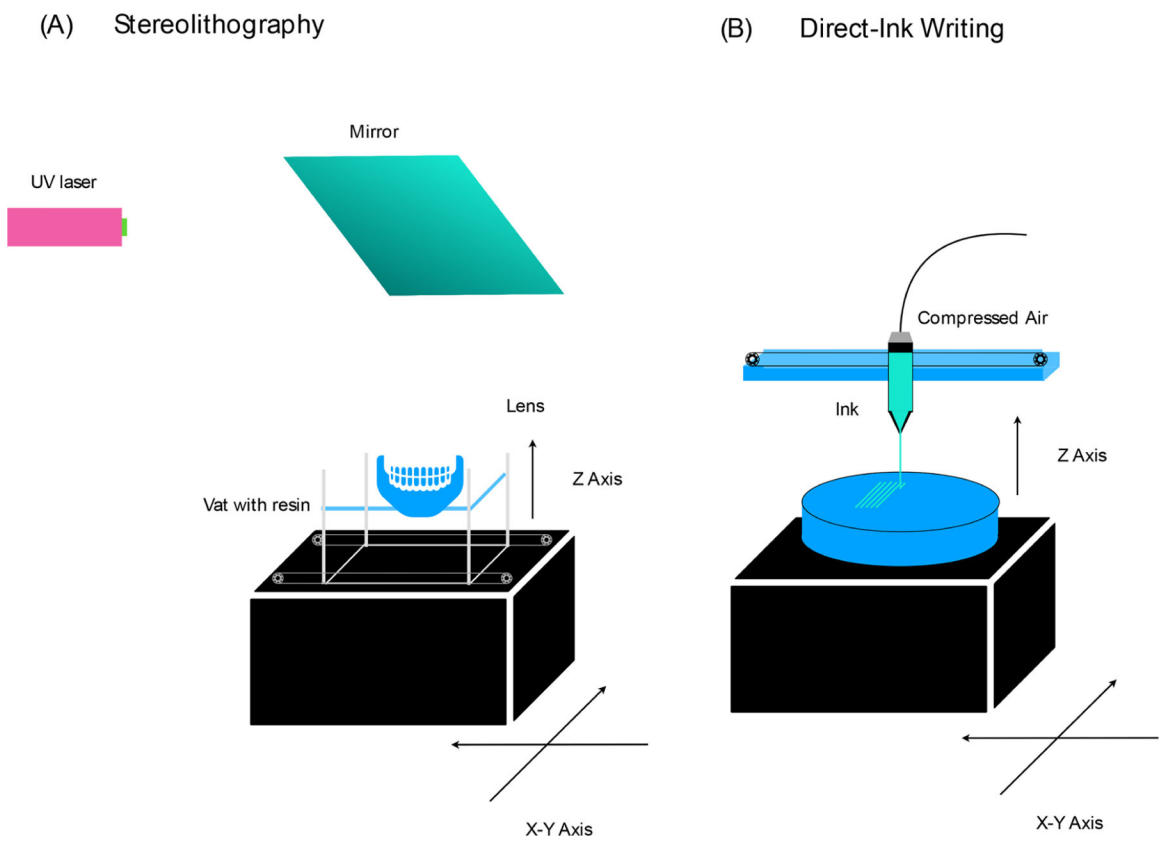

Figure 4.

(A) Schematic representation of stereolithography to create a 3DMD. A UV laser hits a vat filled with resin, resulting in a targeted photopolymerization reaction that allows for material solidification. (B) In DIW, a pressure controller regulates material flow while the nozzle moves in the *x* and *y* planes. Created with BioRender.com.

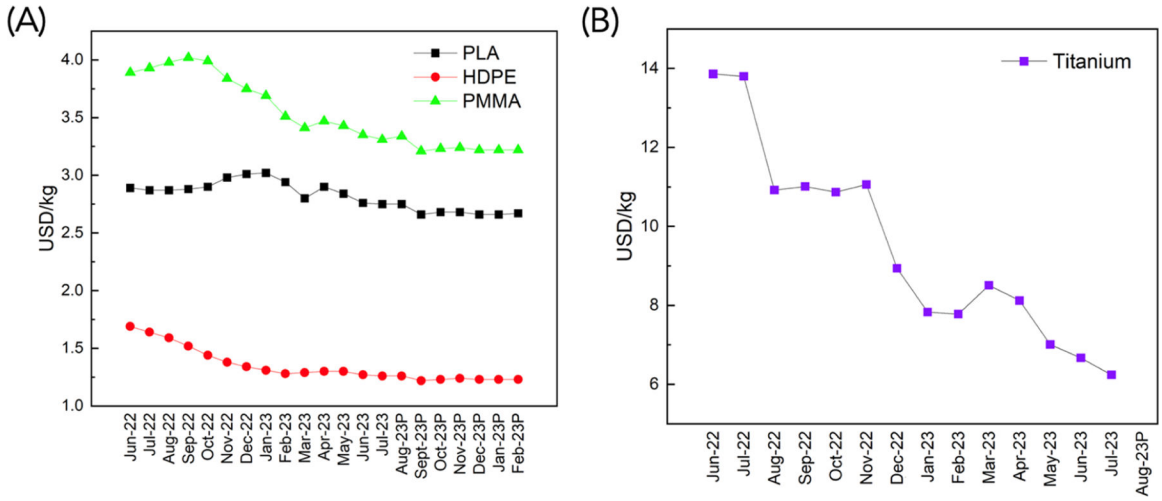

Figure 5.

(A) Cost per kilogram for various thermoplastic polymer raw materials over the past year (until July 2023) with projected values (P) for the next six months. (B) Cost per kilogram for raw titanium over the past year.

Table 1.

Overview of the Most Commonly Used Biomaterials in CMF Repair

Material	Advantages	Disadvantages	Ref
Titanium	Excellent for rigid fixation, strong, lightweight, osteointegrative, resistant to corrosion	Stress shielding and micro- or nano- wear particles may cause implant loosening, metal artifact with imaging that obscures surrounding anatomy	21, 29, 50, 51, 53, 54
Polycaprolactone (PCL)	Cost effective, easily copolymerized with other materials	1–2 years degradation time	21, 87–89
Polylactic acid (PLA)	Nontoxic degradation products, easily copolymerized	Acidity may cause local inflammatory response, degradation time of 6–24 months	11, 91–95
Polyglycolic acid (PGA)	Nontoxic degradation products, easily copolymerized	Acidity may cause local inflammatory response, degradation time of 1.5–3 months	94–99
Polylactide- co-glycolide (PLGA)	Degradation rate is customizable	More expensive	91, 95, 97–99
Poly(methyl methacrylate) (PMMA)	Nondegradable and modulus similar to bone	Scarce information about risk ofinfection	100–106
Polyethylene (HDPE)	Nondegradable, highly durable, inexpensive	Risk of infection and extrusion	80, 107, 109
Polyetheretherketone (PEEK)	Nondegradable, modulus similar to bone, autoclavable without risk of deformation	Possible risk ofseizure and extrusion when used in cranioplasty	72, 111–114
B-Tricalcium phosphate (B-TCP)	Osteointegrative, osteoinductive, and osteoconductive	Brittle, slow degradation rate, poor angiogenic properties	25, 83, 116–118

Table 2.

Trailing 12 Months of Reported Volatility (Standard Deviation) and % Change Per Month of Cost per Kilogram of Each Material

Material	Volatility	% Change per Month
PLA	$0.08	−0.36%
HDPE	$0.15	−2.22%
PMMA	$0.26	−1.21%
Titanium	$2.48	−5.57%

Table 3.

Summary of Recent CMF Applications of Patient-Specific 3D Printed Anatomical Models

procedure name	sample size	patient age	material used	software used	printer used	sterilization	manufacturer	time to manufacture	cost per model	biomedical engineer used	result	complications	ref
Mandibular Oncologic Reconstruction	*n* = 5	18–63 yrs	*a*	Materialise	*a* (SLA)	*a*	*a*	*a*	*a*	Medical Modeling Inc.	Excellent bone-to-bone approximation, decreased intraoperative time and measurements, symmetric mandibular contour	None	188
Maxillary Oncologic Reconstruction	*n* = 16	26–85 yrs	Acrylic resin	SurgiCase CMF	*a* (SLA)	*a*	*a*	*a*	*a*	Medical Modeling Inc.	Prebent reconstructive locking plate, orthogonal jaw relationships	None	187
Mandibular Reconstruction (osteomyelitis)	*n* = 1	51 yrs	PLA, Formlabs white resin	3DSlicer, Autodesk MeshMixer	Form 2 Formlabs (SLA)	*a*	*a*	35 h	*a*	*a*	Prebent plates, decreased intraoperative time, improved accuracy of surgery	None	192
Midface Distraction (hemifacial microsomia syndrome)	*a*	*a*	*a*	Mimics, Materialise, 3matic	3D System Zprinter 650 (MultiJet)	*a*	*a*	7.4 h (complete skulls), 6.0 h (maxillofacial)	$61 (complete skulls), $40 (maxillofacial)	*a*	Subjective decreased intraoperative time, prebent plates, more thorough patient consultation	None	189
Face Vascularized Composite Allotransplantation	*n* = 1	21 yrs	Multimaterial	TeraRecon, Magics	Stratasys J750 (PolyJet)	*a*	*a*	28.2 h, 13.8 h	$762 (recipient), $695 (donor)	Cleveland Clinic Biomedical Engineering Department	Furthered understanding of spatial anatomy, improved education, but time-consuming	None	214
Craniofacial Reconstruction	*n = 2*	10–34 yrs	PLA	Rapid3D, De-Vide	MakerBot Replicator (FDM)	Hydrogen peroxide and gas plasma (Sterrad)	*a*	14 h	$25	*a*	Improved surgical accuracy	None	190

procedure name	sample size	patient age	material used	software used	printer used	sterilization	manufacturer	time to manufacture	cost per model	biomedical engineer used	result	complications	ref
Cleft Lip and Palate Reconstruction	*n* = 30	*a*	ABS (bone) + TangoPlus (soft tissue)	Mimics	Fortus 3D Printer + Connex 3D Printer (PolyJet)	*a*	*a*	*a*	*a*	*a*	Improved patient education and satisfaction	None	215
Frontal Craniotomy and Bilateral Orbitotomy[b]	*n* = 1	1.5 yrs	Multimaterial	Mimics	*a* (PolyJet)	*a*	*a*	38 h	*a*	*a*	Preoperative surgical practice and better impression of anatomic characteristics	None	216
Auricular Reconstruction (microtia)	*n* = 1	*a*	PLA	Amira + Blender,	Builder Premium 3D Printer (FDM)	Autoclave	*a*	4 h (Print only)	$1.10 (material), $501 (material and labor)	*a*	Greater repetitions to practice carving auricular framework, reduced estimation when shaping the ear	None	150
Craniosynostosis Repair	*n = 2*	0.5–2 yrs	Clear resin	Mimics	*a* (SLA)	Standard per institutional protocol	*a*	*a*	*a*	*a*	Merging of patient anatomy with normative anatomy and Intraoperative contouring of the calvaria on anatomic model	None	191
Mandibular Distraction Osteogenesis	*n* = 5	7–10 yrs	PLA	3DSlicer, Cura Software	*a* (FDM)	*a*	*a*	2 h	$25	Dremel 3D Idea Builder	Prebending of osteosynthesis material, improved learning for trainees	None	194
Rhinoplasty	*n* = 12	16–59 yrs	PLA	Blender	Builder Premium 3D Printer (FDM)	Autoclave	*a*	44 h	$5	*a*	Improved patient education and expectation setting, good intraoperative comparison to visualize desired outcome	None	193

procedure name	sample size	patient age	material used	software used	printer used	sterilization	manufacturer	time to manufacture	cost per model	biomedical engineer used	result	complications	ref
Orbital Osteotomy[c]	$n = 1$	11 yrs	*a*	*a*	HP DesignJet 3D	*a*	*a*	*a*	*a*	*a*	Osteosynthesis material was precontoured on the 3D model	None	217

[a] Not applicable.

[b] Frontoethmoidal meningoencephalocele.

[c] Orbital hypertelorism.

ACS Biomater Sci Eng. Author manuscript; available in PMC 2024 July 08.

Table 4.

Summary of Recent CMF Applications of Patient-Specific 3D Printed Surgical Guide

procedure name	sample size	patient age	material used	software used	printer used	sterilization	manufacturer	time to manufacture	cost	biomedical engineer used	result	complications	ref
Craniosynostosis Repair	$n = 4$, $n = 5$	0.75–6yrs, 0.66–1.33yrs	*a*, Polyamide	Materialise, 3D Slicer + Free-form Plus + CranioNav	*a* (SLA, SLS)	*a*, Autoclave	*a*	*a*	*a*	Medical Modeling Inc,*a*	Decreased intraoperative time and reduced irregularities from preoperative osteotomy design and bone shaping, improved accuracy via repeated guide placement registration	None, None	218, 219
Facial Transplantation	$n = 2$	*a*	Appropriate medically approved plastic	Planmeca Romexis, 3D-Systems Geomagic Freeform	*a*	*a*	*a*	8 h	*a*	*a*	Decreased surgical time and simplified bony reconstruction	None	220
Nasal Prosthesis Insertion	$n = 1$	58yrs	ABS	NobelGuide, Amira 3.1.1, Rapidform XOS2, Rhino 3.0	Stratasys (FDM)	*a*	*a*	*a*	*a*	*a*	Accurate implant positioning and easier accessibility for hygienic maintenance	None	151
Neonatal Mandibular Distraction Osteogenesis	$n = 1$	0yrs	*a*	Medical Modeling	*a*	*a*	*a*	*a*	*a*	*a*	Proper fit of cutting guides led successful placement of device	None	221
Maxillofacial Reconstruction	$n = 9$	*a*	*a*	*a*	*a*	*a*	Stryker, Synthes	*a*	*a*	Materialise, KLS Martin	Higher proportion of bone segment contact and successful reconstruction of more subunits	None	222

ACS Biomater Sci Eng. Author manuscript; available in PMC 2024 July 08.

procedure name	sample size	patient age	material used	software used	printer used	sterilization	manufacturer	time to manufacture	cost	biomedical engineer used	result	complications	ref
Mandibular Reconstruction	*n* = 38	~51.0yrs	Polymer	SurgiCase SMF, Materialise	[a] (SLA)	[a]	[a]	[a]	[a]	Medical Modeling Inc.	Reduced operative time and improved reconstructive accuracy	None	197
Forehead Contouring	[a]	[a]	[a]	ProPlan CMF 3.0, 3-matic	[a]	[a]	[a]	[a]	[a]	Materialise	Mock surgery with guides and model allowed for optimal surgical planning	None	223
Soft Tissue Correction via Fat Grafting	*n = 6*	[a]	Biocompatible photopolymerizing resin	Mimics, Zbrush	Form 2 (SLA)	[a]	[a]	[a]	[a]	[a]	Quantifiable volume and location for facial filling leading to better patient outcome	None	196
Cranial Vault Reconstruction	*n* = 3	28–41yrs	[a]	Anatomage In-Vivo, Rhinoceros	[a] (SLA)	[a]	[a]	[a]	[a]	[a]	Reduced intraoperative time	None	28
Mandibular Step Osteotomy	*n* = 1	21yrs	Titanium	Mimics, Simplant Pro	[a]	[a]	[a]	[a]	[a]	[a]	Prevention of injury to adjacent structures, reduced operative time, and improved surgical outcomes	None	31

[a]Not applicable.

Table 5.

Summary of Recent CMF Applications of Patient-Specific 3D Printed Implants

procedure name	sample size	patient age	material used	software used	printer used	sterilization	implant manufacturer	time to manufacture	cost	postoperative follow-up	result	complications	ref
Nasal Septal Deformity Reconstruction	$n = 14$	~38 ± 11 yrs	PCL (pore size: 500 μm)	*a*	*a*	Gamma Irradiation	*a*	*a*	*a*	$T = 3$ mo and ~4 yr	Long-term clinical efficacy and safety, maintenance of mechanical strength	None	198
Primary Reconstruction of Fronto-orbital Region	$n = 1$	13 yrs	PEEK	*a*	*a*	*a*	*a*	*a*	*a*	$T = 2$ mo	Some left-sided temporal hollowing, overall optimal aesthetic and safe results in fronto-orbital reconstruction	None	199
Orbital Wall or Maxilla-orbital Reconstruction	$n = 26$ 3D: $n = 12$ Stock: $n = 14$	~42 yrs	3D: Ti6Al4V ELI Stock: Ti6Al4V ELI	Pro/ ENGINEER (PTC)	Arcam (EBM)	*a*	Planmeca	*a*	*a*	$T = 0$ mo	Average decrease of operation time in 3D vs Stock Orbital: ~ 0.4h maxilla-orbital: ~ 3.82h	Implant incorrect shape due to error in CAD ($n = 2$)	200
Subperiosteal Implants for Atrophic Mandible	$n = 10$	~70 yrs	Ti6Al4V ELI	Mimics (Materialise), Studio 2012 (Geomagics), Meshmixer (Autodesk)	ProXDMP100, 3D System (DMLS)	*a*	IUXTA-3D (BTK)	2–3 weeks	*a*	$T = 12$ mo	100% survival rate, surgeon-determined good to excellent adaptation and fit	Implant incorrect shape due to scattering from nearby crowns in CT ($n = 2$)	201
Cranioplasty	$n = 21$	~28.6 yrs	Ti6Al4V ELI	3-Matic, Magics (Materialise)	Arcam A1 (EBM)	*a*	*a*	*a*	*a*	$T = ~14.1$ mo	Patients satisfied, good fixation of implants, and satisfactory symmetry	Infection + implant removal ($n = 1$)	209
Cranioplasty	$n = 38$	~43 ± 18 yrs	PEEK	Maxilim (Medicim NV), 3ds	*a*	*a*	*a*	*a*	*a*	$T = 6$ mo	Comparable complication rates to literature on	Infection + removal ($n = 5$), hematoma ($n = 4$), CSF	210

procedure name	sample size	patient age	material used	software used	printer used	sterilization	implant manufacturer	time to manufacture	cost	postoperative follow-up	result	complications	ref
				Max 2012 (Autodesk)							auto- or allograft cranioplasties. In 3 pts with infection, implant was successfully removed and reused after sterilization	leak (n = 1). wound-re-lated (n = 1)	
Cranioplasty	n = 6	~46 ± 21 yrs	PEEK	a	a	a	DePuy Synthes	~2 wks	$8493 ± $837.98	T = 4 yr	Good surgical outcomes with high patient satisfaction	None	211
Cranioplasty	n = 11	~46 yrs	PEEK	a	a	a	DePuy Synthes	a	a	T = ~6 mo	Satisfactory aesthetic results overall	None	212
Cranioplasty	n = 8	~44 yrs	Hydroxyapatite (pore size: 300 and 550 um)	a	a (SLA)	Gamma irradiation	3DCeram	2–3 weeks	$10,640 to 13,300* (adjusted for inflation)	T = 1, 6, and 12 mo	Satisfactory aesthetic results overall	None	213
Maxillofacial Reconstruction	n = 24 mandibular: n = 14 zygomatic: n = 3 orbital: n = 7	~30.8 yrs	PEEK	a	a	a	DePuy Synthes + Planmeca	a	a	T = ~16.2 mo	Fit to surrounding bone was perfect in 22 cases, yet outer contour of implant modified in 9 cases prior to fixation. Infection rate of 8.3% comparable with 3D printed PEEK studies	Wound dehiscence (n = 2)	114
Maxillary Reconstruction	n = 32	28.63 yrs	Ti6Al4V ELI	a	a	a	Planmeca	a	a	T = 0 mo	Precise fitting of all implants except one	Implant incorrect shape due to error in mandible position during CT (n = 1)	202

procedure name	sample size	patient age	material used	software used	printer used	sterilization	implant manufacturer	time to manufacture	cost	postoperative follow-up	result	complications	ref
Maxillary or Mandibular Reconstruction	*n* = 33 3D: n = 17 Stock: *n* = 16	3D: 56 ± 14 yrs; Stock: 55 ± 16 yrs	Grade 2 titanium	ProPlan CMF 2.0, 3-Matic 13.0 (Materialise)	*a* (SLM)	*a*	*a*	*a*	*a*	*T* = 0 mo	3D: superior accuracy of reconstructive outcomes No difference in total operative time between 3D and stock groups	3D: None Stock: Exposure + removal (*n* = 2)	203
Isolated Mandibular Advancement ± LeFort I Maxillary Osteotomy	*n* = 60; mandibular: *n* = 30; mandibular + maxillary: w = 30	~27 yrs	Grade 2 titanium	ProPlan CMF (Materialise)	*a* (SLS)	*a*	Materialise	*a*	*a*	*T* = 1 mo	No difference between planned and actual position of the mandible in either group when considering absolute values of the differences	*a*	204
Maxillary ± Mandibular Osteotomies	*n* = 43 3D: n = 18 Stock: *n* = 15	~23 yrs	3D: Titanium Stock: *a* (Stryker)	*a*	*a*	*a*	*a*	*a*	*a*	*T* = ~9.8 mo	Reduced operative time in 3D maxillary/ stock mandibular plates subgroup vs 3D maxillary/3D mandibular and stock maxillary/ stock mandibular plate groups without significant difference in complications	3D: Infection (*n* = 3) + removal (*n* = 2), palatal fistula + repair (*n* = 1) Stock: Infection (*n* = 2) + removal (*n* = 1), exposure + removal (*n* = 1), occlusal relapse irevision (*n* = 2)	205
Mandibular Anterior Subapical Osteotomy (MASCO)	*n* = 11	~27 yrs	Ti6Al4V ELI	ProPlan CMF 3.0 (Materialise)	*a*	*a*	Materialise	*a*	*a*	*T* = 0 mo	High degree of accuracy between the virtual plan and immediate postoperative result	None	206

procedure name	sample size	patient age	material used	software used	printer used	sterilization	implant manufacturer	time to manufacture	cost	postoperative follow-up	result	complications	ref
Mandibular Contour Reconstruction	$n = 2$	~37 yrs	Ti6Al4V ELI (pore size: 750–950 μm)	Meshmixer Ver. 3.5 (Autodesk), Magics (Materialise)	MetalSys250 (SLM)	*a*	*a*	*a*	*a*	$T = 6$ mo	Patients satisfied, surgical accuracy and postoperative stability without positional change of implant	None	207
Mandibular Contour Reconstruction	$n = 21$ 3D: $n = 9$ Stock: $n = 12$	*a*	3D: PEEK Stock: porous PE (MED P OR, Stryker)	3D-Surgery (*a*)	*a*	*a*	*a*	*a*	*a*	$T = 0$ mo	Reduced operative time and greater facial symmetry in 3D group	3D: Infection ($n = 2$) Stock: Infection ($n =$ l)	208

*a*Not applicable.

ACS Biomater Sci Eng. Author manuscript; available in PMC 2024 July 08.